Politecnico di Torino

Master of Science in Building Engineering
A.Y. 2025/2026
March 2026

Rainwater Harvesting Potential in Residential Blocks in Turin:

Comparative Study of Green and Traditional Roofs

Relatore:
Prof.ssa Ilaria Butera
Correlatori:
Ing. Matteo Carollo

Candidate:
Anastasiia Simanushkina

CONTENTS

ABSTRACT

At the scale of individual buildings, rainwater harvesting (RWH) performance can be precisely estimated using water balance modeling, which accounts for rainfall input, storage dynamics, and water demand. However, the evaluation is usually more complex at an urban scale, due to the high building heterogeneity and a lack of detailed information on each building characteristics and number of inhabitants.

In this study, a GIS-supported methodology, integrated with behavioral modeling, is used to evaluate RWH potential at the building block scale. The analysis has been applied to a residential area of Turin, Italy. The specific study area covers over 0.6 km^2 and is predominantly composed of typical residential blocks representative of the city's urban fabric. Within these boundaries, a total of 52 residential building blocks were identified, each containing at least one building of residential use and at least one inhabitant, since this work focuses on domestic non-potable water use only. The selected area serves just as a spatial framework for integrating building and demographic data, but the main calculations are done at the building block level.

Building blocks were classified according to roof area per inhabitant, and representative blocks from dominant classes were selected for detailed modeling. RWH performance in terms of non-potable water savings and rainwater retention efficiency was evaluated for both traditional roofs and green roofs.

In addition, one representative building block was used to assess the operational cost associated with pumping harvested rainwater into the building system. The analysis confirms that the main economic benefit arises from avoided potable water consumption, while the costs of energy use for pumping are negligible. The economic impacts of system installation, maintenance, and energy use should be considered alongside the technical specifications, as they contribute to the overall feasibility and long-term sustainability of the RWH system.

The results demonstrate the potential of RWH in residential building blocks of Turin, showing the influence of roof type, tank capacity, and roof area per inhabitant ratio on system performance. Representative building blocks were analysed to estimate water savings and retention efficiency for both traditional and green roof configurations, allowing comparison of their effectiveness. A conceptual real-scale design illustrates the practical application of RWH in the existing urban environment, while the economic assessment demonstrates the long-term benefits of RWH systems mainly through savings on water costs.

INTRODUCTION

Urban areas are experiencing increasing pressure on water resources due to population growth and climate variability. At the same time, intense rainfall events create stress on urban drainage systems and increase flood risks [Carollo et al., 2022]. Rainwater harvesting (RWH) systems represent a promising strategy that can simultaneously reduce potable water demand and improve stormwater management [Campisano et al., 2017; Notaro et al., 2016].

RWH systems collect, store, and treat rainwater from rooftops and other impervious surfaces for non-potable uses, such as toilet flushing, laundry, irrigation, and cleaning, potentially satisfying a significant fraction of domestic water demand [GhaffarianHoseini et al., 2016; Carollo et al., 2022].

The performance of RWH systems depends strongly on site-specific factors, including roof type, roof area, tank size, occupancy, water demand patterns, and local rainfall characteristics [Campisano et al., 2014; Campisano and Modica, 2015]. High-resolution rainfall and water use data are often required to reliably evaluate tank efficiency and overflow, while simplified approaches based on annual averages can misrepresent performance, especially for stormwater peak reduction [Palla et al., 2012; Jenkins, 2007; Imteaz et al., 2015]. At larger scales, from building blocks to neighborhoods or cities, accounting for spatial variability in roof area and occupancy patterns is crucial to accurately estimate the potential benefits of RWH [Lúcio et al., 2020; Islam et al., 2021].

In this study, we focus on assessing the potential of RWH in residential building blocks in Turin, Italy, comparing traditional and green roof typologies. Using a GIS-supported methodology, residential building blocks are classified by roof area per inhabitant, and representative blocks from dominant classes are selected for detailed modeling using the behavioral model proposed by Lúcio et al., 2020. Rainwater harvesting performance is evaluated for non-potable domestic uses, primarily toilet flushing, for different tank capacities. A conceptual real-scale design of RWH system for one representative block was also performed, illustrating the practical realization of such systems in the existing urban environment. Operational cost for pumping harvested water was analyzed, showing that the main economic benefit comes from avoided potable water use, while energy demand for pumping is negligible.

More resilient urban water management by reducing potable water consumption and mitigating urban runoff supports the United Nations Sustainable Development Goals (SDGs), especially SDG 6 – clean water and sanitation, SDG 11 – sustainable cities and communities, and SDG 13 – climate action.

Nomenclature:

t	time step [s]
V_t	volume of water contained in the tank after the inflows and outflows that occur in interval t [m^3]
Q_t	inflow volume to the tank at time step t [m^3]
Y_t	yielded volume of rainwater from the storage tank at time t [m^3]
O_t	overflow volume [m^3]
R_t	collected rainfall at time step t [m]
φ	rooftop runoff coefficient [-]
ff_t	the first flush diversion [mm]
N_t	net rain volume [m^3]
H	total rooftop area [m^2]
D_t	non-potable water demand [m^3]
S	tank storage capacity [m^3]
α	fraction of rainwater conveyed to the tank before the daily supply [-]
RR_t	volume of the retained rainwater [m^3]
GRR_t	green roof retention [m^3]
Q	annual rainwater volume collected on roof, neglecting the first flush [m^3]
D	annual non-potable water demand [m^3]
E_{annual}	annual pumping energy [kWh/year]
V_{annual}	average annual harvested water [m^3]
$C_{energy\ annual}$	annual pumping operating cost [€/year]
$C_{water\ annual}$	annual water cost [€/year]

1. PROPOSED METHODOLOGY

1.1. Building scale

A RWH system, as illustrated in Fig. 1, consists of four main components. First, a catchment surface (1), typically the building roof. Second, a convey system (2), including gutters and some coarse filters that remove large debris such as leaves and twigs. Third, a storage tank (3). And fourth, a pump system (4) that supplies harvested water to indoor uses or outdoor applications such as gardens and green roofs. When the tank reaches its capacity, any excess of water is discharged to the sewer network through an overflow outlet (5). A mains water top-up line (6), controlled by a level sensor (7), ensures minimum water levels in the tank during dry periods. Since rainfall and water demand rarely coincide in time, the storage tank plays a critical role in balancing these two patterns.

In many cases, rainwater undergoes additional treatment, such as fine filtration or disinfection, immediately before reuse, particularly for domestic purposes in order to reduce health risks [Leong et al., 2017].

The non-potable water volume supplied through RWH depends on local precipitation regimes, tank volume, and the water demand [Carollo et al., 2022]. Across Europe, performance has improved significantly, and several studies in Italy indicated that water-saving efficiencies of 70%–80% can be achieved with modest tank volumes [Liuzzo et al., 2016; Palla et al., 2011].

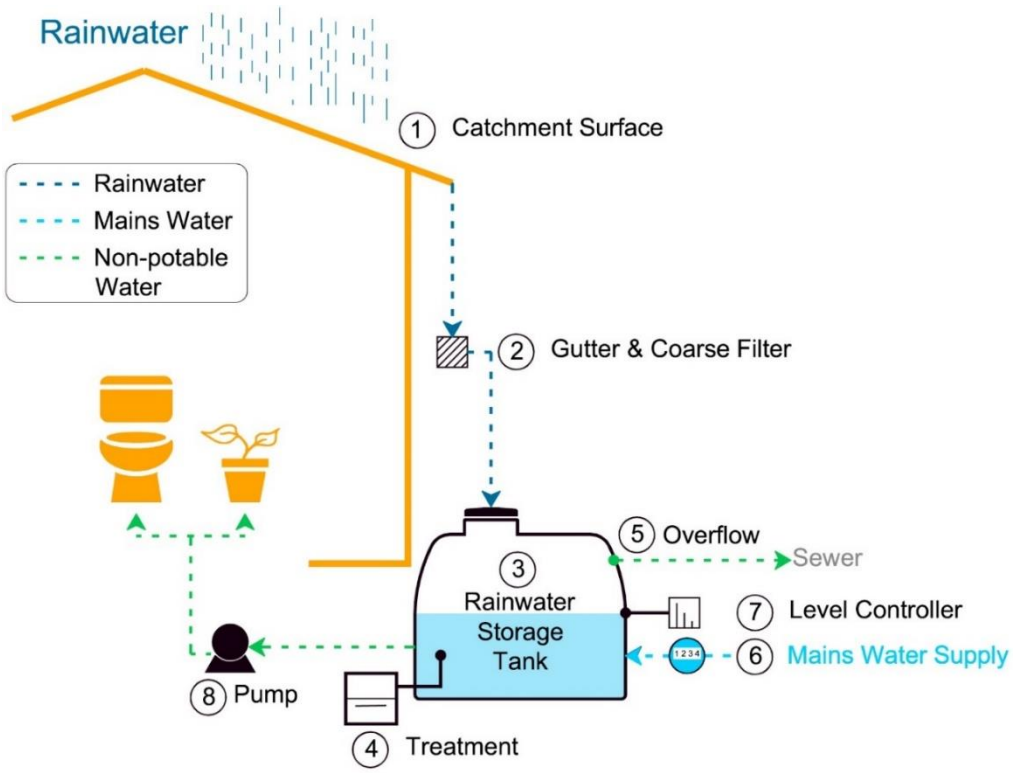

Fig. 1 | Scheme of a domestic rainwater harvesting system [https://doi.org/10.1016/j.spc.2018.09.002]

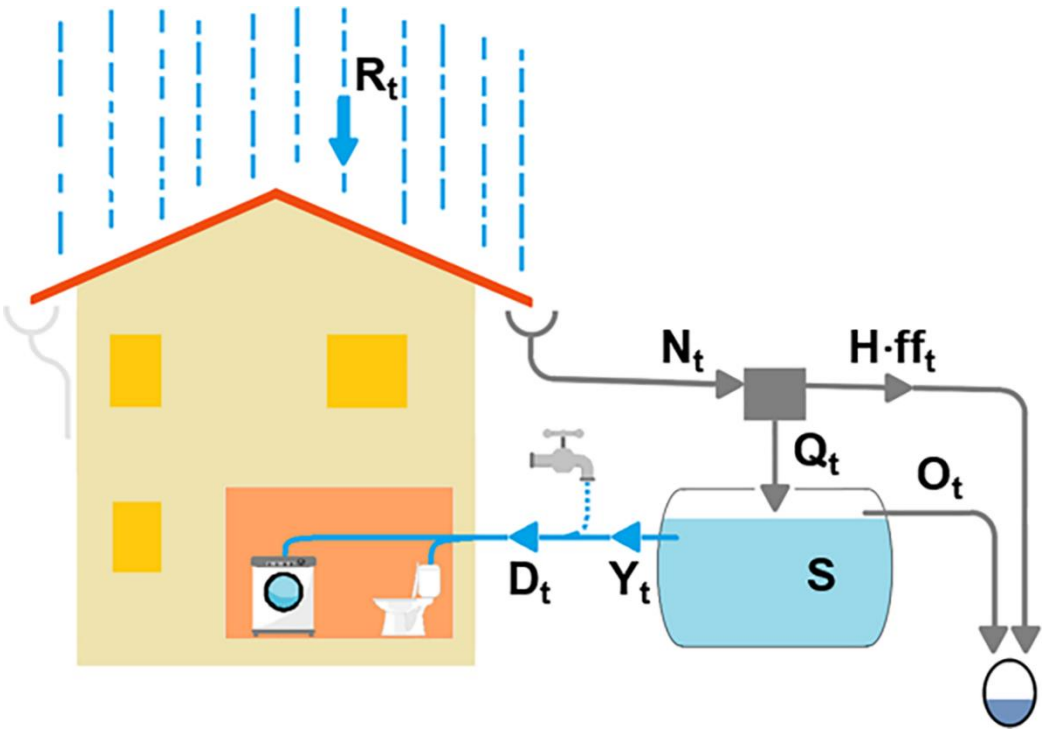

Fig. 2 | Scheme of a domestic rainwater harvesting system with symbols [https://doi.org/10.1371/journal.pone.0278107.g001]

1.2. Performance at the building block scale

Evaluating the performance of RWH systems for each individual building within a district is not feasible due to data and computational constraints. Instead, this study uses an aggregated approach based on "building blocks" – spatial units defined by clusters of adjacent buildings bounded by streets. Each block combines the total roof area of the included buildings and the demographic data of residents obtained from corresponding census sections. This approach allows the assessment of RWH potential at an intermediate scale between individual buildings and the entire district, capturing spatial variability while maintaining computational efficiency.

Each building block is defined by two key parameters: the total roof area (representing the harvesting surface) and the number of inhabitants (representing the water demand). Nowadays, it is possible to identify the roof area of every building using GIS data, while demographic information can be obtained from open-source statistical databases like ISTAT in Italy.

For the sizing and assessment of RWH system efficiency, various approaches exist, ranging from deterministic to statistical ones, each used to estimate system performance and determine appropriate storage capacity (e.g., Fewkes and Butler, 2000; Palla et al., 2011; Lúcio et al., 2020; Guo et al., 2007; Raimondi et al., 2014; Silva et al., 2015).

Among them, the so-called behavioral models, rely on recorded rainfall data and realistic water demand patterns [Ghisi et al., 2007; Mitchell et al., 2007; Brodie et al., 2012; Campisano et al., 2012; Campisano et al., 2013].

They use a finite difference scheme to update the tank volume step by step, following the mass-balance logic. At each interval, the model adds the collected rain, subtracts the supplied demand, and applies the tank limits. This produces a time-resolved simulation of how the system would actually perform under real conditions.

In this paper, we use the behavioral model proposed by Lúcio et al., 2020: unlike the widely used Yield After Spillage (YAS) or Yield Before Spillage (YBS) methods (see Fewkes and Butler, 2000), this model considers that a fraction of the daily inflow is conveyed to the tank before the distribution of the daily water supply.

The core of the model (see Figs 2 and 3) is the following water balance equation for the tank:

$$V_t = Q_t + V_{t-1} - Y_t - O_t \quad (1)$$

where V_t is the volume of water contained in the tank after the inflows and outflows that occur in interval t; Q_t is the inflow volume supplied to the tank at time step t; Y_t is the rainwater volume supplied to the users and O_t is the overflow volume. The subscript t refers to a generic time step, 1<t<T, where T is the total simulation period. Recent work by Campisano et. al. (2014) has shown that the model setup and parameter choices change results in a noticeable way, mainly because tank performance depends on the selected time resolution. Daily steps work for estimating water savings. Hourly steps are needed to assess runoff reduction. Minute-scale data become essential when studying peak flow reduction. In this study, a daily time step is adopted, as the primary objective is the evaluation of long-term water savings and overall system performance rather than short-term runoff dynamics or peak flow reduction. The model is solved through a finite-difference scheme.

Not all rain falling on a roof can be collected in the storage tank, as some is lost to evaporation or declines by the first-flush system to remove low-quality water. As a result, the effective inflow to the RWH tank is lower than the total rainfall depth.

Hence, the inflow to the tank at time step t is computed as:

$$Q_t = (\varphi \cdot R_t - ff_t) \cdot H = N_t - H \cdot ff_t \quad (2)$$

where R_t is the rainfall depth at time step t; φ is the runoff coefficient and ff_t is the first flush diversion. In our case H is the catchment roof area of all buildings inside

the building block. In this way, $N_t = \varphi \cdot R_t \cdot H$ represents the net rain volume available for collection.

In this work, two roof configurations are considered: a traditional roof with a rainwater harvesting (RWH) system and a green roof combined with RWH.

For traditional roofs, runoff generation is described using a constant runoff coefficient φ, typically equal to 0.8, in accordance with UNI/TS 11445 (2012) and previous studies [Farreny et al., 2011]. In this case, evaporation and minor initial losses are implicitly included in the runoff coefficient, while water quality protection is ensured by the first-flush diversion, which varies from 1 to 5 mm per rainy day [Amin et al., 2013, Kus et al., 2010]. In this work it is set to 1 mm.

In the case of green roofs, runoff generation is not assumed constant, as a significant fraction of rainfall can be retained within the substrate and later lost through evapotranspiration.

In this study, the empirical rainfall–runoff model for green roofs developed by Sousa et al., 2025 was adopted. According to it, the first flush was modelled at the rainfall event scale, because (i) the consideration of the total constant runoff coefficient is incompatible with the variable runoff from the green roof, and (ii) it is reasonable to assume that during rainfall events lasting for several days, it is not necessary to subtract the first flush every day. In this context, rainfall events were considered independent if there had been an antecedent dry weather period (ADWP) of at least 24 h. The model is based on linear and non-linear multiple regression analysis calibrated using the experimental dataset by Palermo et al., 2019, which is considered a reference for green roof hydrological modelling in Italy. As reported in Sousa et al., 2025, the empirical models (Table 1) show high goodness of fit, with Adjusted R^2 values up to 0.975.

Therefore, the runoff coefficient for green roof is calculated dynamically as a function of rainfall characteristics and antecedent moisture conditions using the following empirical relationship:

$$\varphi = -0.059 + 0.185 \cdot \ln(P) - 0.068 \cdot \ln(ADWP) \quad (3)$$

where P is the rainfall depth and ADWP is the antecedent dry weather period.

The sign of the regression coefficients is consistent with what was physically expected: (i) a positive sign for the precipitation means proportionally more runoff as the total rainfall of the event increases; (ii) since an increase in duration with the same total precipitation means less precipitation intensity; and (iii) a negative sign

for ADWP, since the moisture content of the soil decreases with the length of the dry period prior to a rainfall event.

Table 1 | Regression models of the runoff and runoff coefficient of the green roof

Table 2 | Regression models of the runoff and runoff coefficient of the green roof

Model	Unstandardized coefficients		Standardized coefficients			95.0% Confidence interval for B	
	B	Std. Error	Beta	t	Sig.	Lower bound	Upper bound
Linear models							
Runoff							
(constant)	1.654	1.701		0.972	0.337	−1.781	5.088
P	0.757	0.024	1.020	31.986	0.000	0.709	0.804
D	−3.462	1.016	−0.109	−3.408	0.001	−5.514	−1.410
LnADWP	−1.677	0.685	−0.072	−2.449	0.019	−3.060	−0.294
Runoff coefficient							
(constant)	−0.059	0.040		−1.498	0.142	−0.139	0.021
LnP	0.185	0.011	0.889	16.516	0.000	0.163	0.208
LnADWP	−0.068	0.014	−0.259	−4.820	0.000	−0.097	−0.040
Non-linear models							
Runoff							
(constant)	15.354	5.263		2.917	0.006	4.726	25.983
P^1.255	0.227	0.006	1.019	38.785	0.000	0.216	0.239
D^0.258	−14.298	5.076	−0.074	−2.817	0.007	−24.548	−4.047
LnADWP^2.035	−0.597	0.158	−0.091	−3.777	0.001	−0.916	−0.278
Runoff coefficient							
(constant)	0.064	0.033		1.941	0.059	−0.003	0.130
ln*P*^1.427	0.087	0.005	0.892	17.088	0.000	0.077	0.097
lnADWP^1.026	−0.070	0.013	−0.275	−5.269	0.000	−0.097	−0.043

$$runoff\ coefficient = -0{,}059 + 0{,}185 \cdot \ln(P) - 0{,}068 \cdot \ln(ADWP)$$

The runoff estimated through the Sousa et al., 2025 model was integrated into a standard mass balance framework to simulate the performance of the RWH system. For green roofs, runoff was estimated using a net-rainfall approach, assuming that retention occurs at the beginning of the rainfall event and is not uniformly distributed over its duration. This approach allows the model to account for the variable runoff characteristic of green roofs, while remaining compatible with large-scale analyses based on daily rainfall data.

The terms Y_t and V_t in Eq (1) are computed with the following algorithm [Lúcio et al., 2020]:

$$Y_t = \min\begin{Bmatrix} D_t \\ V_{t-1} + \alpha \cdot Q_t \\ S \end{Bmatrix} \text{ and } V_t = \min\begin{Bmatrix} V_{t-1} + Q_t - Y_t \\ S - Y_t + (1-\alpha) \cdot Q_t \\ S \end{Bmatrix} \quad (4), (5)$$

where the non-potable water demand D_t depends on the usage patterns, while the coefficient α represents the fraction of rainwater conveyed to the tank before the daily demand (ranging from 0 to 1). Preliminary results obtained by Carollo et. al., 2022 indicated that, in their study of Turin districts, the α value has minimal impact on the RWH performance indices. Based on this, we set $\alpha = 0.5$, meaning that half of

the net rainwater volume collected on the roof is conveyed to the tank before the daily supply.

To evaluate the performance of rainwater tanks two key indicators widely adopted in the literature [Mitchell et al. 2008; Campisano et.al. 2014] were calculated in this study: non-potable water saving efficiency E_{WS} [%] and volumetric retention efficiency E_R [%].

The water-saving efficiency of a rainwater harvesting system quantifies the proportion of non-potable water demand that can be met using harvested rainwater instead of mains supply [Dixon et al., 1999].

$$E_{WS} = \frac{\sum_{t=1}^{T} Y_t}{\sum_{t=1}^{T} D_t} \cdot 100 \quad (6)$$

In other words, a higher E_{WS} value means a greater share of non-potable water is replaced by rainwater. And 0% means the system supplies no rainwater and all demand is met by mains water.

Different tank capacities are considered, and the minimum capacity should respect the $S/Q \geq 0.01$ constraint, as a daily time step is used [Fewkes Aet al., 2000].

As storage volume increases, E_{WS} rises rapidly at first, then approaches an asymptotic maximum as additional increases in tank size provide progressively smaller gains. Achieving the theoretical maximum efficiency would require exceptionally large tanks, which are often impractical from both spatial and economic standpoints.

For domestic uses, design practice usually accepts a water-saving efficiency below the theoretical maximum. Following the Italian Standard (UNI/TS 11445) an initial estimate of the storage volume can be taken as 10% of the smaller value between annual inflow Q, calculated using the runoff coefficient and the presence of first flush in case of traditional roof, while for green roofs it is derived from the average annual runoff depth, and annual non-potable water demand D. This preliminary size is then checked against a performance criterion: the resulting E_{WS} should reach at least 80% of the maximum achievable efficiency. If not, the tank capacity is incrementally increased until this threshold is met.

Volumetric retention efficiency measures how effectively the RWH system (and green roof if present) holds back rainwater to reduce downstream stormwater runoff, either across the catchment surface or into the sewer system. It is calculated using the following equation [Sousa et al., 2025]:

$$E_R = \frac{\sum_{t=1}^{T} RR_t}{H \cdot \sum_{t=1}^{T} R_t} \cdot 100 \quad (7)$$

where $RR_t = Y_t + GRR_t$ – the rainfall retained. The green roof retention for time step t – $GRR_t = (1 - \phi_t) \cdot Rt \cdot H/1000$.

However, achieving 100% retention efficiency for traditional roof was not possible due to the presence of the first flush diversion.

In the case of combined green roof-RWH system, a retention efficiency of 100% can be achieved because the roof system significantly reduces runoff generation.

2. APPLICATION TO THE AREA OF THE CITY OF TURIN, ITALY

2.1. Case study

The present study focuses on a selected area within the city of Turin, Italy, as a representative case for testing the proposed tool, building upon previous research on the topic (e.g., Carollo et al., 2022). Turin, the capital of the Piemonte Region, is located in northern Italy at an average elevation of about 240 meters above sea level. According to the Köppen–Geiger climate classification [Beck et al., 2023], the city falls within the Cfa category, characterized by a humid subtropical climate with hot summers and mild winters.

The municipality of Turin covers approximately 130 km² and hosts about 848,748 inhabitants [ISTAT, 2021].

For the city of Turin, the most recent demographic and spatial data were obtained from the Piemont region geoportal. The dataset contains polygons representing census sections (*sezioni di censimento*), which are sub-municipal territorial units further subdividing the statistical zones (i).

The geometries are valid from 02/12/2024, and the associated information is periodically updated according to the revision date provided.

According to Istituto Nazionale di Statistica (ISTAT, 2021) the municipality of Turin is divided into 94 statistical zones (Fig. 3). AperTO, the open data portal of the City of Turin, defines statistical zones as intramunicipal territorial units formed by a group of census areas, used to organize demographic and spatial data within a municipality. Each statistical zone is further subdivided into census sections, representing smaller urban blocks composed of several adjacent buildings.

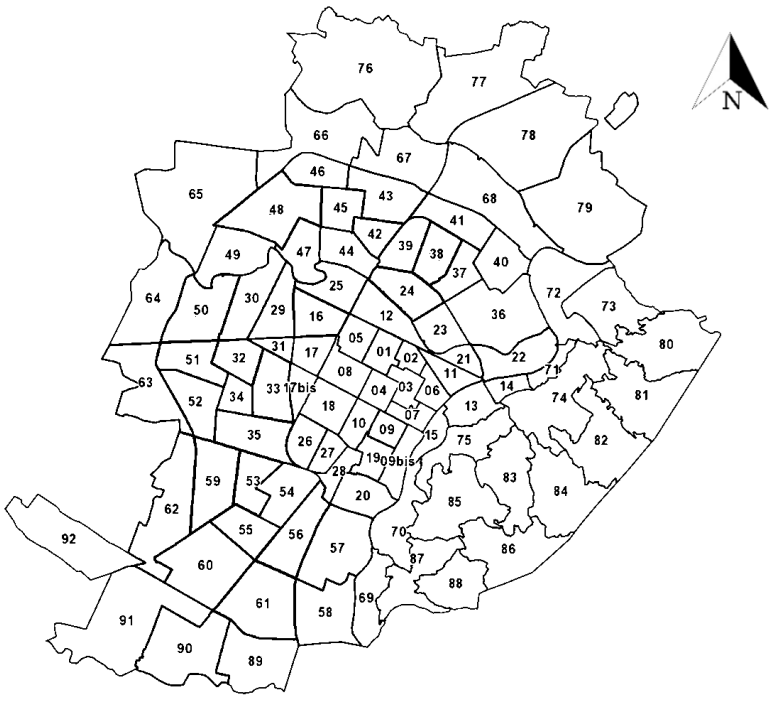

Fig. 3 | Statistical Zones (*zone statistiche*) of Turin [ISTAT, 2021]

To take advantage of existing databases, in this research Statistical Zone 26 (Fig. 4) was selected as the case study area. The specific study area extends over 654,020 m^2, as calculated in ArcGIS, and is predominantly composed of typical residential blocks representative of the city's urban fabric. The area is bounded by Corso Luigi Einaudi to the north, Corso Galileo Ferraris to the east, Via Giuseppe e Antonio Carle to the south, and Corso Mediterraneo to the west. Within these boundaries, a total of 797 building units were identified.

Most of the buildings in this sector have pitched roofs with a moderate slope, commonly finished with traditional terracotta tiles, which are characteristic of Turin's architectural style. This typology reflects the city's post-war residential development and provides a consistent morphological setting for the study.

For each census section, the dataset provides demographic indicators such as the resident population, number of families, number of dwellings and the number of buildings used for residential purposes.

By spatially overlapping this dataset with another GIS layer containing information on the building roof area footprints, it is possible to estimate the catchment surfaces available for RWH. This integrated spatial approach allows for the identification of representative urban blocks and supports the simulation of RWH systems' performance at different scales within the city.

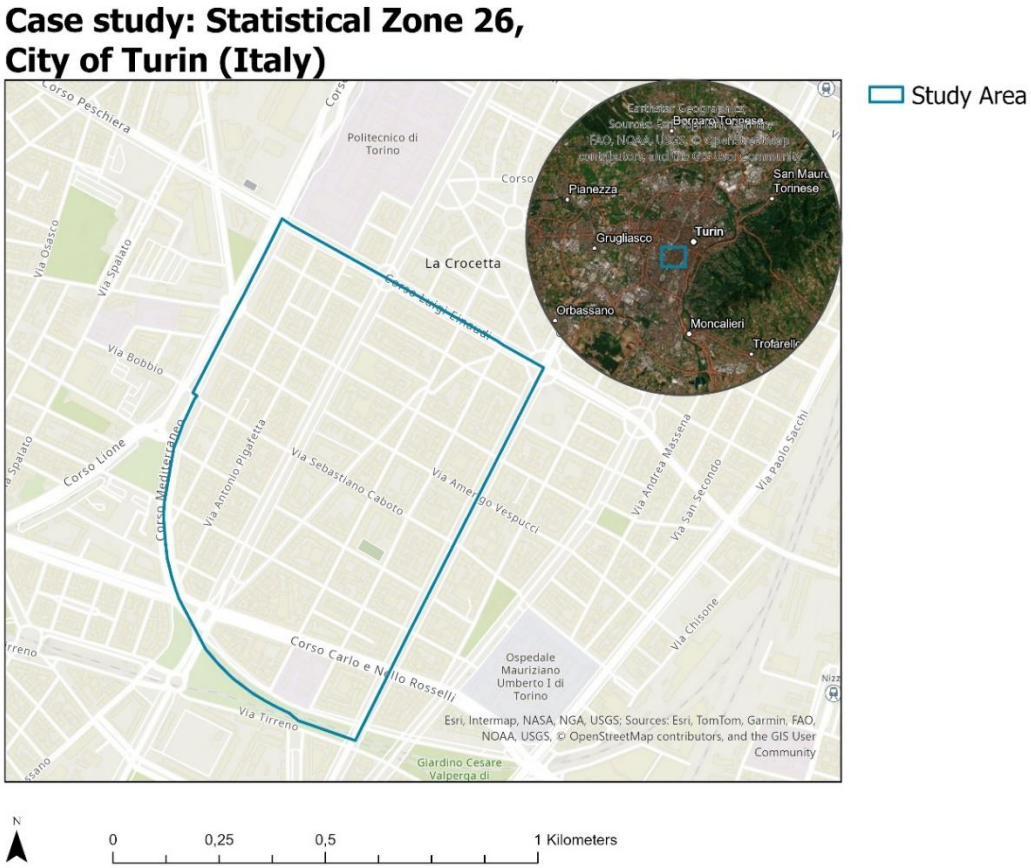

Fig. 4 | Case study: Statistical Zone 26, City of Turin (Italy)

Since the study focuses exclusively on non-potable domestic water demand, sections without inhabitants or without residential buildings were excluded from the analysis. Fig. 5 represents all census sections within our study area, while in Fig. 6 only census sections containing at least one residential building and one inhabitant are shown. Excluded sections generally correspond to non-residential areas, such as roads or specific institutional and commercial buildings, including:

- Section ID 1196: Istituto Comprensivo Ugo Foscolo (school);
- Section ID 5991: RSA La Trinite' (building for nursing services);
- Section ID 5939: Parrocchia di Santa Teresa di Gesù Bambino (Catholic church);
- Section ID 1179: Salesians Crocetta – Istituto Internazionale "Don Bosco" (religious institution);
- Section ID 1157: Scuola Elementare Coppino (elementary school);
- Section ID 5878: Scuola Materna Municipale "Borgo Crocetta" (kindergarten);
- Section ID 5924: Carrefour supermarket (commercial building);
- Section ID 5925: Clinica Pinna Pintor (clinic);
- Section ID 5890: Parrocchia della Beata Vergine delle Grazie (Catholic church).

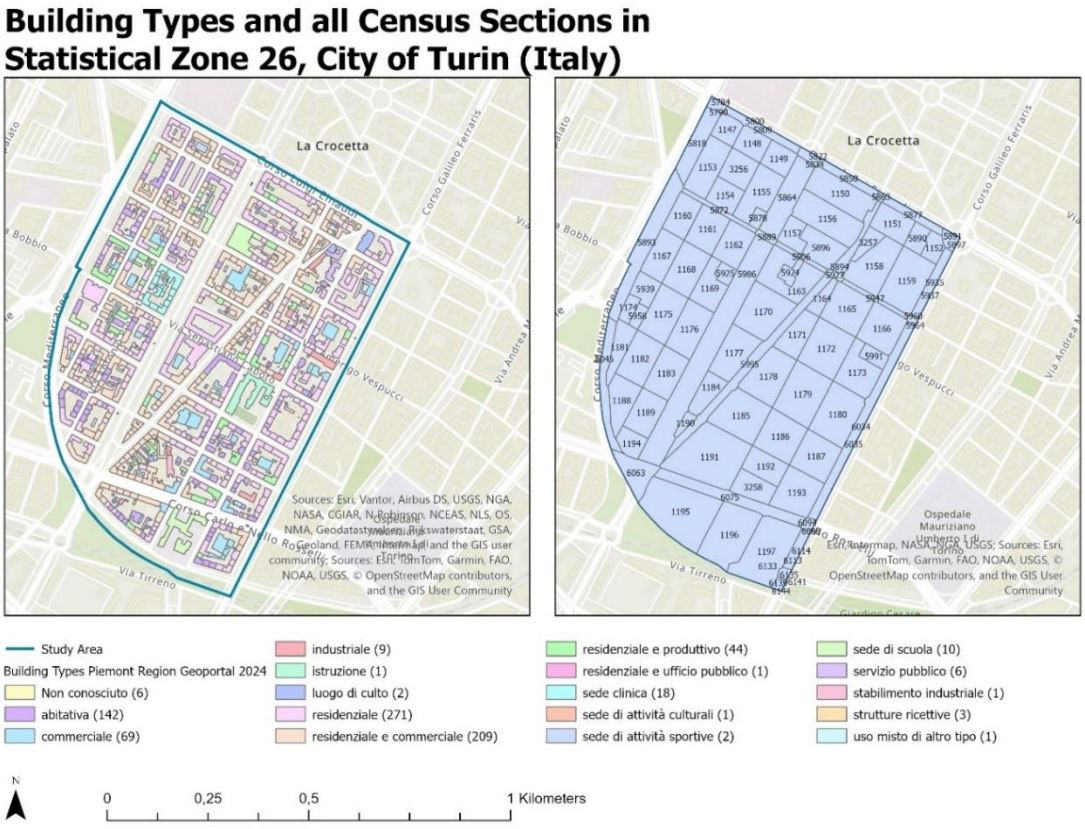

Fig. 5 | Distribution of building types and all census sections in Statistical Zone 26, City of Turin (Italy)

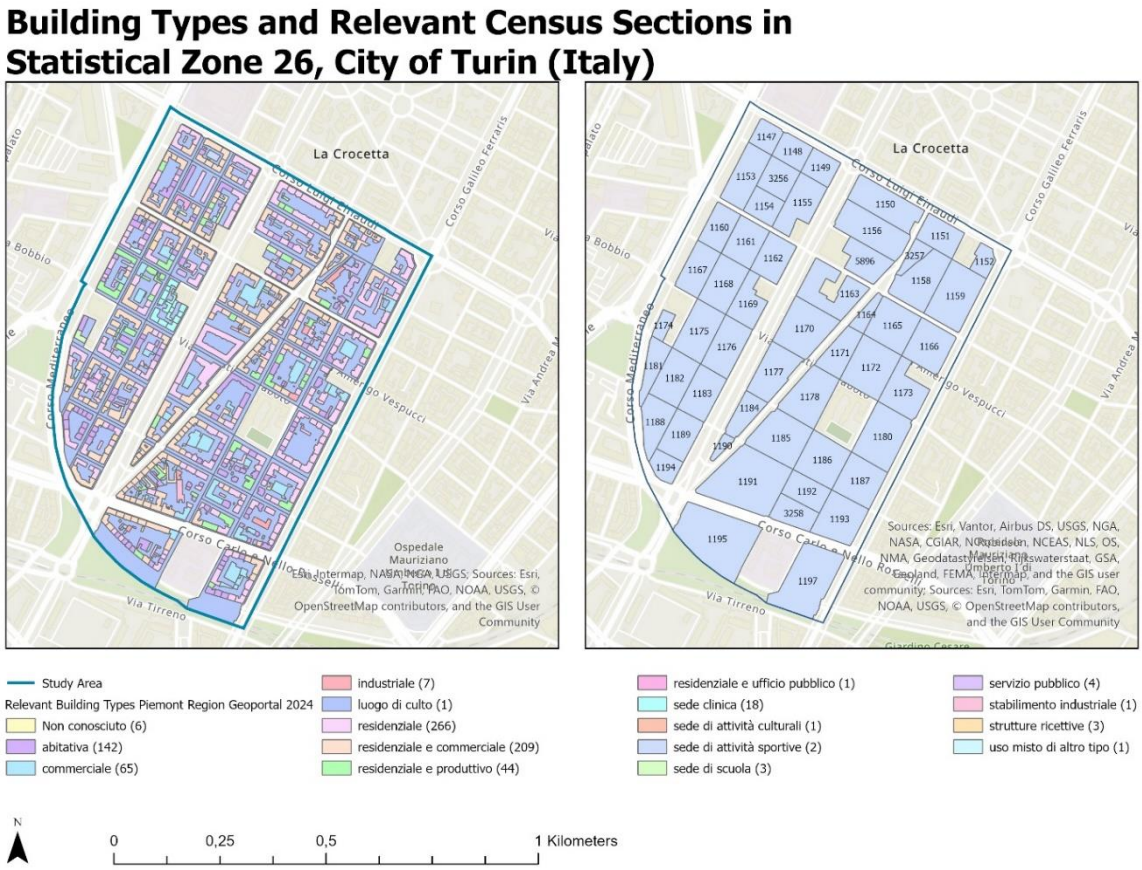

Fig. 6 | Distribution of building types and relevant census sections in Statistical Zone 26, City of Turin (Italy)

2.2. Building block classification and selection of representative cases

To account for the heterogeneity of the urban fabric, building blocks were classified based on the ratio of roof area to the number of inhabitants. The ratio was discretized using a step of 5 m² per inhabitant, creating multiple classes that group blocks with similar characteristics. Three representative classes were identified, covering 92% of all building blocks containing at least one residential building and one inhabitant.

Within each class, a representative building block was selected based on proximity to the class median of the roof area per inhabitant ratio, ensuring that the chosen block reflects the typical characteristics of the class. These representative blocks were then used for detailed RWH performance modeling. Both traditional roof configurations and combined systems integrating green roofs were considered.

The full classification of all building blocks is provided in Table A.1 in Appendix A, while the presented building block classes and the selected representative blocks and their characteristics are reported in the tables below in this section (Tables 2 and 3) and on the map (Fig. 7).

Table 2 | Presented building block classes

CLASS	ROOF/INHAB. LIMITS [m²/pers.]	№ OF RESIDENTIAL BUILDINGS [units]	FREQUENCY [%]
3	10-15	7	13.46%
4	15-20	30	57.69%
5	20-25	11	21.15%
6	25-30	3	5.77%
7	30-35	1	1.92%
	Total	52	100.00%

Table 3 | Selected representative blocks

BUILDING BLOCK ID	ROOF AREA [m²]	INHABITANTS [pers.]	ROOF/INHAB. [m²/pers.]
1195	7211.83	592	12.18
1183	4286.25	247	17.35
1147	2093.84	95	22.04

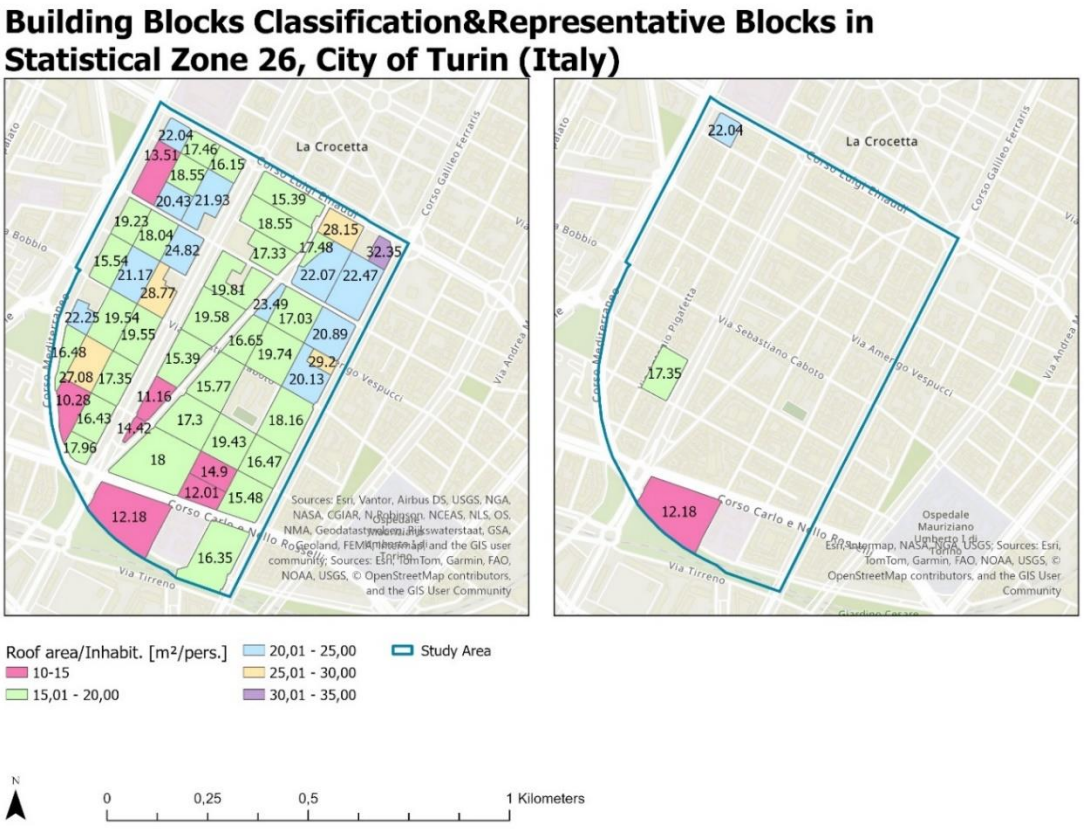

Fig. 7 | Building blocks with roof/inhab. ratio.
Left: All relevant building blocks. Right: Representative building blocks

2.3. Water consumption

According to the Turin public water utility, the invoiced annual potable water consumption in 293 municipalities of Turin commune with 2,187,721 number of residents in 2024 was 162 mln m^3 [SMAT Bilancio consolidato e d'esercizio 2024]. Per capita domestic consumption averaged 159 l/inhab/day. The non-potable water fraction was estimated to be one-third of the total consumption [Carollo et al., 2022] and equal to 53 l/inhab/day.

2.4. Precipitation regime

The precipitation regime of the study area is analysed based on rain data collected at the rain-gauge station in the city of Turin with a most close to our case-study elevation above sea level. Based on measurements taken from Google Earth, the elevation at the relevant road intersections ranges from 246 to 250 m above sea level, and an average elevation of 248 m was used in the analysis.

Among all rain-gauge stations listed in the databases of the Regional Agency for Environmental Protection in the municipality of Turin, the most appropriate station is "Torino Via della Consolata" station, located at 244 m above sea level and situated within 3 km of the study area. This station offers continuous daily precipitations record from 19/12/2003 to the present, with no missing days. Considering only complete calendar years, the period from 01/01/2004 to 31/12/2024 was selected, resulting in 21-year simulation dataset based on the availability of continuous short-time-step rainfall data.

In general, a minimum of 30 years of continuous rainfall data is recommended to ensure a robust and reliable performance assessment of RWH systems (e.g., Palla et al., 2011; Geraldi&Ghisi, 2018). However, many raingauge stations in and around the city of Turin do not have a collection of climatic data going back this far.

Researchers have used rainfall time series of varying lengths depending on data availability. The literature includes analyses based on 25-year series (e.g., Agudelo-Vera et al, 2013; Basinger et al., 2010), 10-year series (e.g., Herrmann&Schmida, 2000; Villarreal&Dixon, 2005), and even 1–7-year series (e.g., Ghisi et al., 2012). Several studies directly compared short and long time series with 30-50-year benchmarks and found that datasets of 10 years or longer can reproduce long-term results reasonably well, though this depends strongly on climate and the performance metric (e.g., Mitchell, 2007; Geraldi&Ghisi, 2017, 2018). These conclusions agree with WMO,1989 guidance, which considers 10-year rainfall records sufficient to represent average rainfall characteristics.

A consistent finding across the literature is that higher rainwater demand amplifies the differences between short and long series. Under high demand, the same collected volume supplies a smaller fraction of total use, making system

performance more sensitive to climate variability. Analyses across multiple cities [Geraldi&Ghisi, 2018] showed substantial variability: climates with very low or very high annual rainfall produced larger deviations, whereas moderately wet cities such as Quebec showed stable results. Similar patterns appear in broader climate studies, which emphasize that rainfall distribution within the year can influence simulation outcomes as much as total annual rainfall [Imteaz et al., 2015; Moniruzzaman&Imteaz, 2017] and recommend incorporating seasonality indices [Jenkins, 2007].

Despite this variability, most studies converge on the conclusion that 10–15-year rainfall series generally provide results comparable to 30-year series regarding potable water savings and optimal tank sizing. A lower threshold of about 7-10 years is also supported by climate research, since such intervals typically capture at least one full cycle of major climate oscillations such as El Niño and La Niña [Domeisen et al., 2013]. Therefore, for practical RWH design, rainfall series of roughly a decade or longer represent a reasonable compromise between accuracy and data availability.

The annual rainfall values for all years in the 2004-2024 period at the "Torino Via della Consolata" station are illustrated in Fig. 8, and no statistical evidence of any trend was found. In that way, although some studies show that there will be a variation in the hydrologic regime due to climate changes (e.g., IPCC 2007; Lehner et al., 2006; Frich et al., 2002; Klein Tank et al., 2002), in the present research, these values were considered to represent the hydrologic regime in the near future and no climate changes scenarios are taken into account.

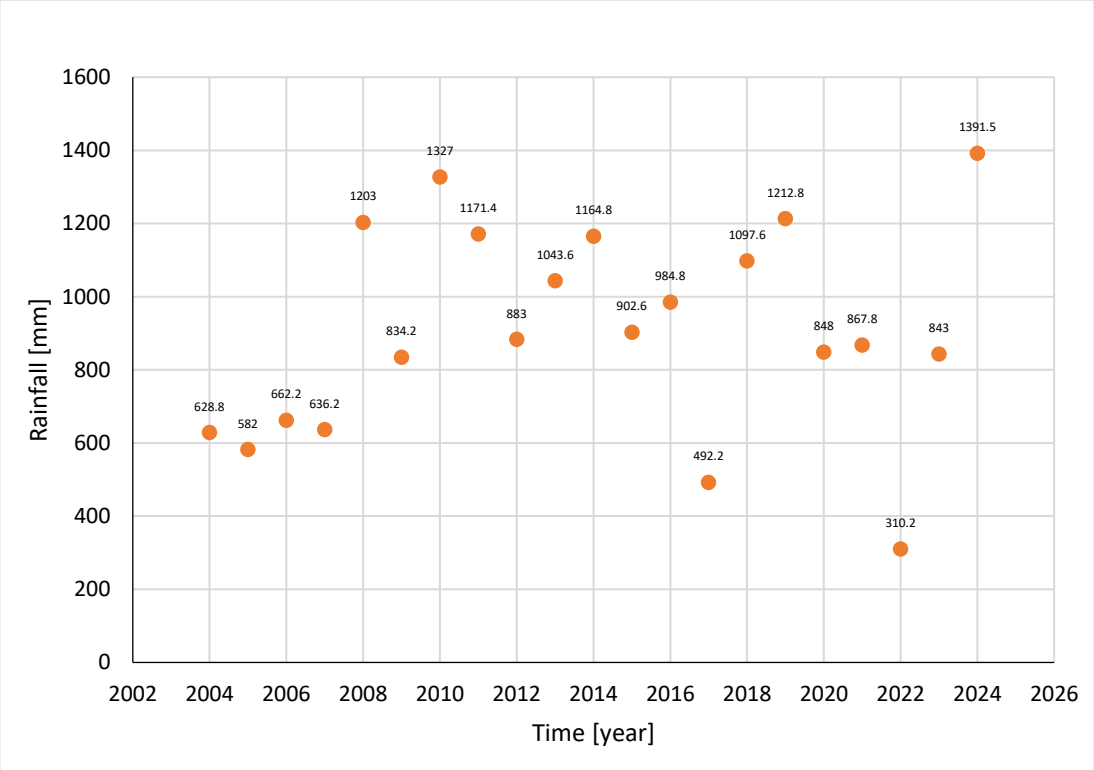

Fig. 8 | Annual rainfall depth at "Torino Via della Consolata" station

2.5. The best tank design and RWH systems performance

The tank volumes were selected after a series of simulations, as explained in Section 1.2.

In this scenario, all the building blocks in the study zone have been considered to be equipped with a tank, and domestic use of the rainwater has been assumed.

A 21-year-long rainfall pattern was considered for the simulations for the district, using the data collected at "Torino Via della Consolata" rain-gauge station managed by the regional Environmental Protection Agency (ARPA).

RWH system performance was evaluated separately for each building block defined in Table 3, through the calculation of the parameters defined in "Proposed methodology" section: (i) non-potable water savings E_{WS}, (ii) rainwater retention efficiency E_R.

Following Farreny et al., 2011, the relation between the pitched roofs orientation and the wind direction was neglected and a runoff coefficient of 0.80 was adopted.

The first flush for traditional roof was assumed to be 1 mm based on the findings by Amin et al., 2013.

The best tanks were distributed throughout the study area in the following way:

- For class 3 which represents 13.46% of all building blocks inside the study area – with traditional roof 255 m^3 and 270 m^3 in case of green roof;
- For class 4 (frequency 57.69%) – 200 m^3 in both cases;
- For class 5 (frequency 21.15%) – 130 m^3 in case of traditional roof and 120m^3 with green rood.

2.6. Performance assessment

The evolution of the non-potable water savings and rainwater retention efficiencies with tank volume for the representative building blocks of three class types is presented in Figs 9 and 10, respectively. These simulations were done with reference to non-potable water consumption without seasonality.

The parameters that mainly affect the water saving efficiency of a building block are the tank capacity and the harvesting area per capita, $H_{pc} = H/P$, which is proportional to the ratio between the rainwater availability and the water demand.

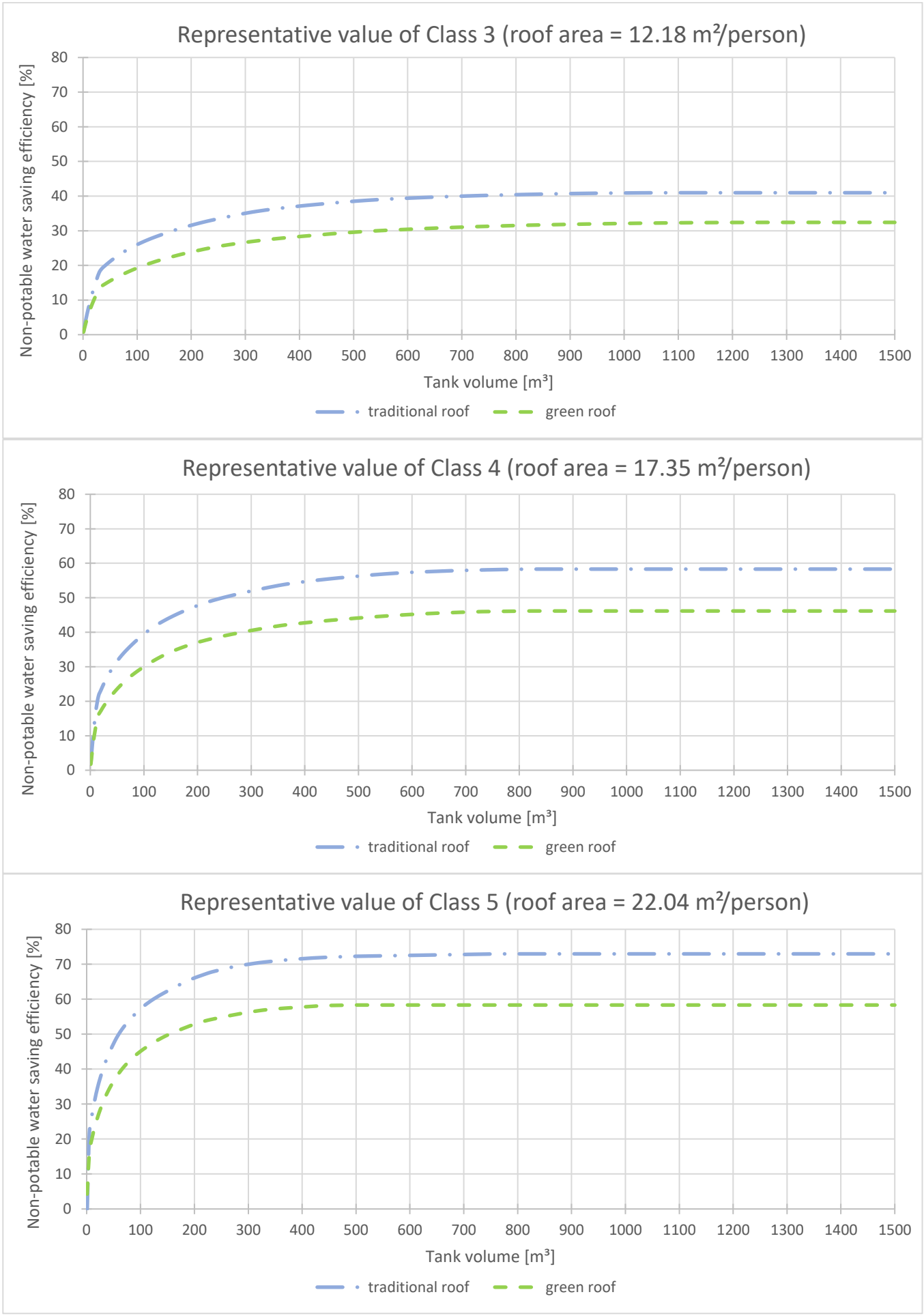

Fig. 9 | Non-potable water savings efficiency of RWH for representative building blocks of classes 3, 4 and 5

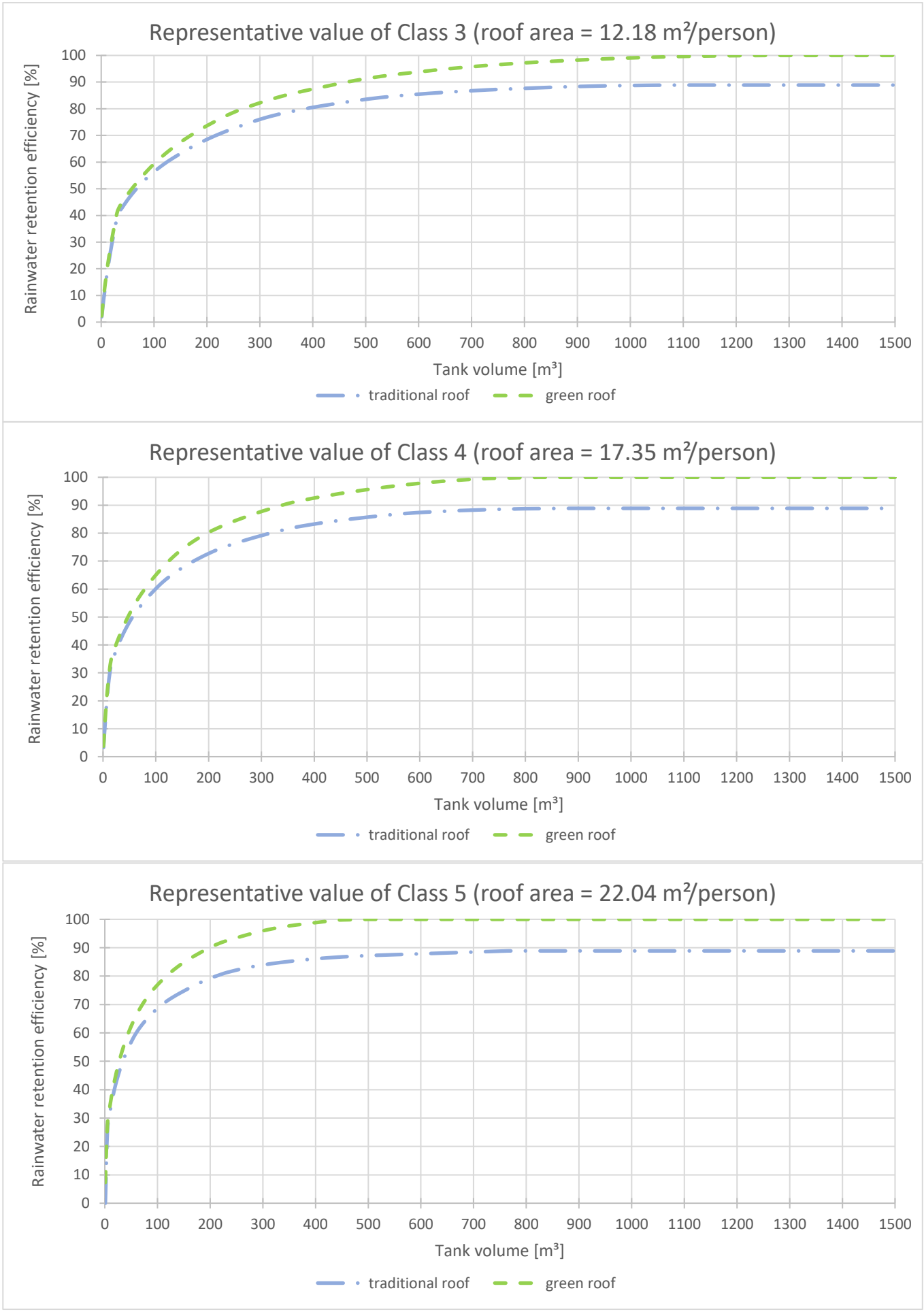

Fig.10 | Rainwater retention efficiency of RWH for representative building blocks of classes 3, 4 and 5

For all building block classes, E_{WS} increases rapidly at small tank volumes and gradually approaches a plateau as storage capacity increases. This behaviour indicates that, beyond a certain tank size, water savings become limited by rainfall availability and non-potable demand rather than by storage capacity. From a financial perspective, the viability of the RWH system decreases when the slope of the relation between tank capacity and the non-potable water savings or rainwater retention efficiency becomes flatter, because it shows that the benefit from investing in a larger tank delivers a smaller increase in benefit.

Across all classes, traditional roofs consistently achieve higher water-saving efficiencies than green roofs. This difference is explained by the rainfall retention capacity of green roofs, which reduces the volume of runoff entering the RWH system and therefore limits the amount of water available for non-potable uses.

Among the compared building blocks, the one with a roof area of 22.04 m^2/person, representing Class 5 (20–25 m^2/person), shows the highest water-saving efficiencies, followed by Class 4 and Class 3. This trend reflects that the increasing roof area per capita ratio results in a higher availability of harvested rainfall relative to non-potable demand.

Fig. 10 illustrates the rainwater retention efficiency E_R for the same building blocks and roof configurations.

For all classes, retention efficiency increases sharply at low tank volumes and then asymptotically approaches its maximum value as tank capacity increases, indicating a decrease in profitability for oversized storage tanks. Green roofs consistently outperform traditional roofs in terms of retention efficiency.

The representative block of Class 5 again exhibits the highest retention efficiencies, followed by Class 4 and Class 3, confirming the influence of roof area per capita.

The results reveal a clear trade-off between maximising non-potable water savings and enhancing rainfall retention. Traditional roofs favour higher water reuse, whereas green roofs significantly improve runoff retention at the expense of reduced water availability for reuse. Therefore, the selection of roof configuration and tank volume should be guided by the primary objective of the system, whether water supply substitution or stormwater management.

Although the efficiencies increase as the tank capacity increases, an important aspect is the distance between the blue and the green lines in Figs 9 and 10, which represents the relative performance of the green roof compared to the conventional roof.

Considering Fig. 9, as the storage capacity of the RWH system increases, the non-potable water savings efficiency loss due to the green roof increases (distance

between the two lines). The reason is that the green roof retains and evapotranspires part of the rainfall, reducing the amount of water reaching the storage tank. While this reduction is less critical for small tanks, it becomes more significant when larger storage volumes are available and could otherwise be fully utilized. For retention efficiency (Fig. 10), when the storage tank is small, the green roof provides a substantial additional retention effect. However, as tank capacity increases, the tank itself is able to retain a larger fraction of runoff, thereby reducing the relative contribution of the green roof.

These results indicate that the benefits of the green roof are higher for small tank volumes.

3. CONCEPTUAL REAL-SCALE TANK DESIGN

3.1. Case study definition and design assumptions

The representative block of Class 5 (20–25 m^2/person), with a roof area of 22.04 m^2/person, was selected for the real-scale design. This block was chosen because it is the most compact and presents fewer internal constraints compared to the other classes representative blocks, where additional constructions are located within the courtyard. Its spatial configuration makes it more suitable for the installation of rainwater harvesting infrastructure.

Two design scenarios are analysed: (i) a traditional roof scenario and (ii) a green roof scenario.

Both scenarios aim to reflect the existing real conditions as closely as possible, given the available data.

For the traditional roof scenario, only roof slopes oriented toward the inner courtyard are considered available for rainwater harvesting. It is assumed that runoff is collected exclusively from these inner slopes, as external slopes typically discharge toward public streets and are not realistically connectable to a courtyard-based storage system.

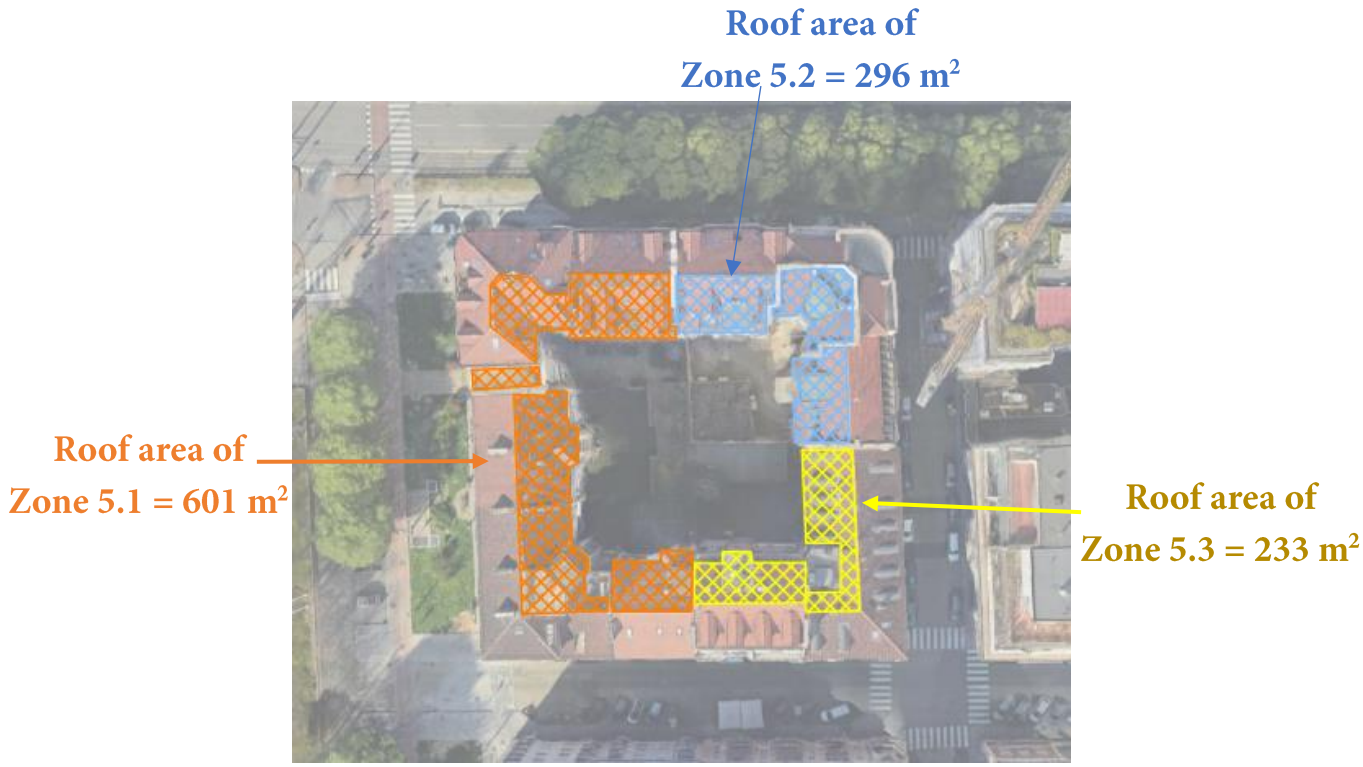

Fig. 11 | Roof areas available for rainwater harvesting in the Class 5 representative building block for the traditional roof scenario

The effective roof area available for collection was measured using Google Earth imagery and is estimated at approximately 1130 m^2. To address spatial constraints in the courtyard, three separate collection zones were identified based on the roof layout:

- Roof area of Zone 5.1: 601 m^2;
- Roof area of Zone 5.2: 296 m^2;
- Roof area of Zone 5.3: 233 m^2.

For the green roof scenario, roof orientation is not a limiting factor. However, implementation is constrained by the presence of roof windows and photovoltaic panels. Only roof sections without such obstacles are considered feasible for green roof installation. Two suitable zones were identified, with areas of 484 m^2 and 348 m^2, respectively. Runoff from remaining traditional roof sections is excluded from the analysis due to uncertainty in downpipe distribution and occupant allocation among buildings.

Fig. 12 | Roof areas suitable for green roof implementation in the Class 5 representative building block

3.2. Subsurface and installation constraints

The rainwater tank is planned to be installed underground to preserve courtyard usability, reduce visual impact, protect collected water from temperature fluctuations, and allow gravity-based collection from roof downpipes. The first step in the design process is to assess site-specific subsurface constraints, including stratigraphy and groundwater conditions, which directly influence excavation feasibility, tank stability, and potential buoyancy risk.

Based on ARPA GeoPiemonte 2021 map (Fig. 13), the site is characterised by Quaternary fluvial and fluvioglacial deposits of Middle to Upper Pleistocene age, composed predominantly of gravel and sand. These coarse-grained, non-

metamorphic sediments are typical of alluvial environments within the western Po Basin and generally provide good bearing capacity. From a design perspective, the relatively high mechanical strength of sandy–gravelly soils are favourable for underground storage tank installation, provided that proper compaction and bedding preparation are ensured. However, their high permeability implies significant hydraulic conductivity, making groundwater conditions a critical design parameter.

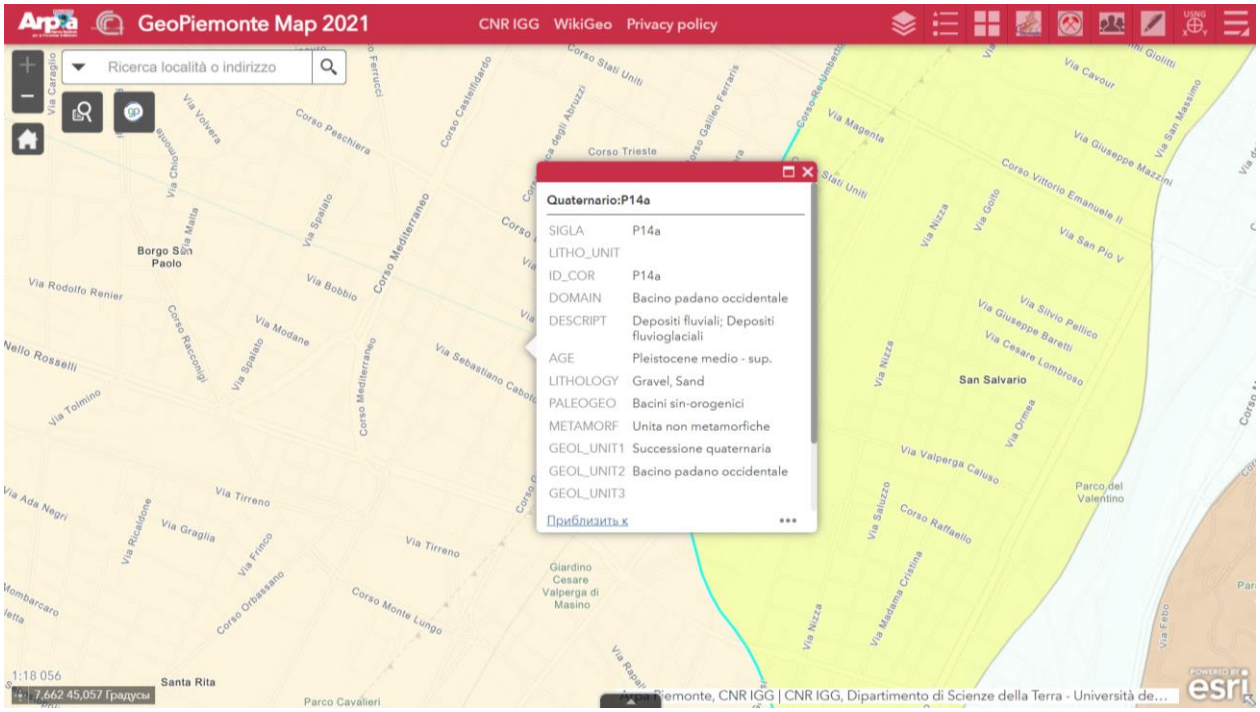

Fig. 13 | Stratigraphic map of the study area showing Quaternary fluvial and fluvioglacial deposits [ARPA GeoPiemonte, 2021]

According to ARPA groundwater monitoring, the closest hydraulic point to the study area is groundwater body GWB-S3b (monitoring point code 00127210001) in Torino (P26 Torino piazza d'Armi). The chemical status of the shallow aquifer is classified as poor. On the latest available date 31/12/2024 at 16:00, the groundwater depth was recorded at 21.76 m below ground level.

This information is essential for evaluating excavation depth, potential groundwater inflow, and buoyancy risks, as well as for determining if anchoring or drainage measures are necessary. For the relatively small storage tanks considered in this study, the site conditions are generally suitable, and no extensive measures are required.

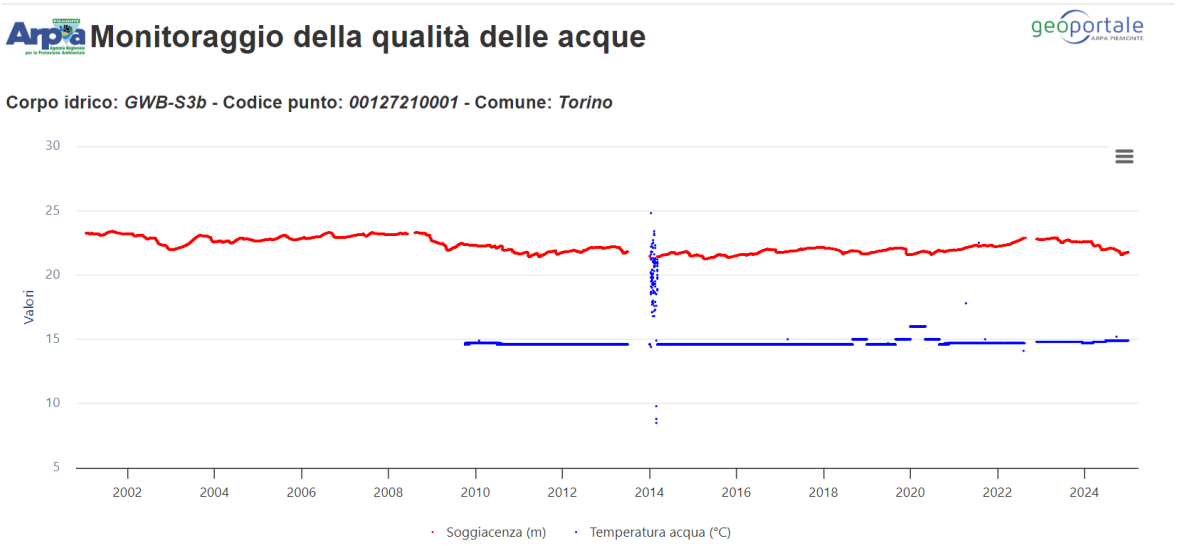

Fig. 14 | Groundwater monitoring point GWB-S3b near the study area showing aquifer depth (red) and water temperature (blue) [ARPA groundwater monitoring]

3.3. Tank sizing and spatial allocation

Based on the available roof area and the representative performance curve (Fig. 15), the maximum E_{WS} efficiency for the traditional roof scenario is 40%. Achieving 80% of this maximum value (32%) requires a total tank capacity of 40 m³. However, by accepting a minor reduction of 5 percentage points (from 32% to 27%), the required volume can be halved to 20 m³. This represents a more cost-effective and practically feasible solution.

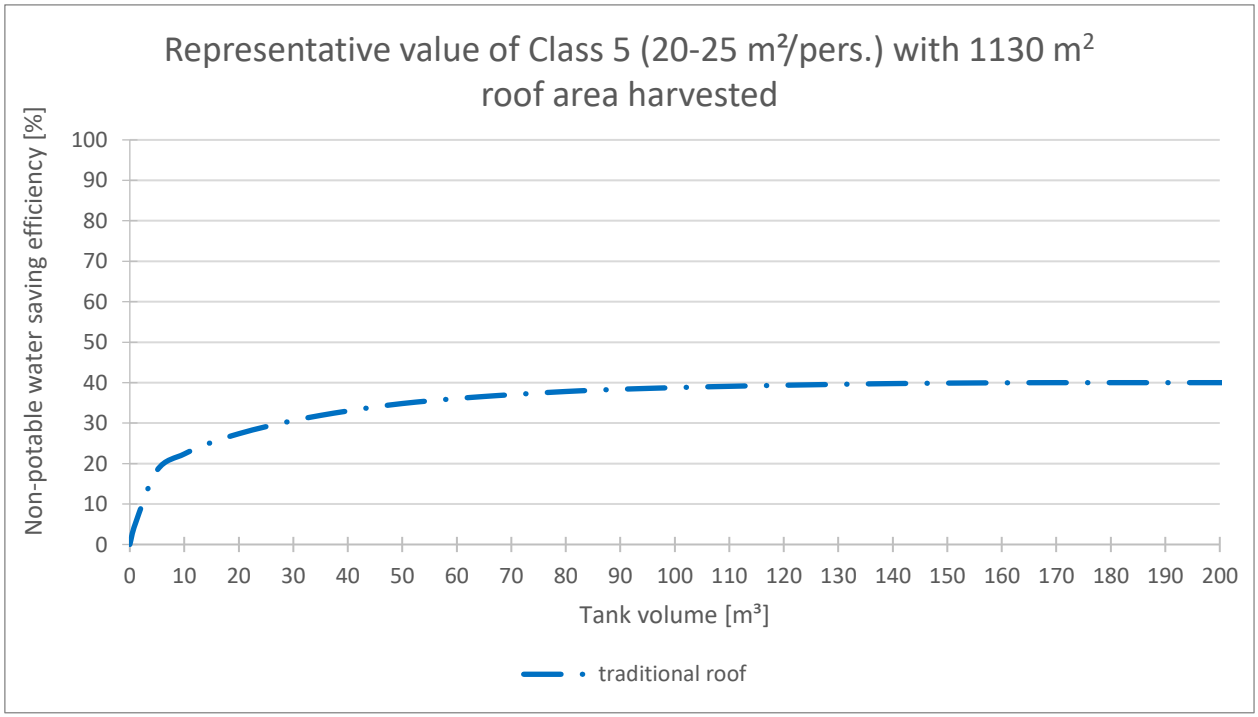

Fig. 15 | Non-potable water savings efficiency E_{WS} for the Class 5 building block under the real traditional roof scenario

The ideal configuration would be to place one water tank at the center of the courtyard and connect all downpipes from the surrounding buildings to it. However, an on-site spatial assessment shows that the courtyard cannot be fully utilized for the installation of rainwater storage infrastructure due to geometrical and functional constraints, primarily the presence of existing low-rise buildings. In addition, the courtyard is divided by partitions into three zones, which may correspond to different ownerships. As a result, it is not feasible to install a single centralized 20 m^3 storage tank and connect all roof downpipes to it.

In practice, the exact amount of water collected by each downpipe cannot be determined, and the number of residents in each building is also unknown, as buildings differ in height and layout. Therefore, for academic purposes, the total required tank volume of 20 m^3 is allocated according to the percentage of roof area for each section (from section 3.1):

- Zone 5.1: ~53% → tank volume ≈ 10,6 m^3;
- Zone 5.2: ~26% → tank volume ≈ 5,2 m^3;
- Zone 5.3: ~21% → tank volume ≈ 4,2 m^3.

A possible design option would be to connect the tanks in series at their base to allow water exchange and improve efficiency; however, as prefabricated tanks are used in this study, such connection is not feasible. Maintenance of the downpipes leading to the tanks remains challenging, as they are located at the tank bottom, requiring partial emptying for inspection or cleaning. For performance evaluation, the roof area is assumed to be approximately evenly distributed among the three tanks.

Using the product catalog of the Austrian company Geoplast, suitable underground polyethylene, double-walled, truck-accessible tanks were selected for each section:

- Zone 5.1: 1 tank of 10 m^3;
- Zone 5.2: 5.2 m^3.;
- Zone 5.3: 4.2 m^3.

This configuration closely follows the proportional roof area distribution while using commercially available tank sizes.

Due to limitations in the Google Earth imagery, the exact locations of existing downpipes cannot be precisely determined; therefore, for simplicity, one downpipe for each building entrance is assumed for the analysis.

Fig. 16 shows the pipe layout. The pipe layout is schematic and does not represent a fully engineered system.

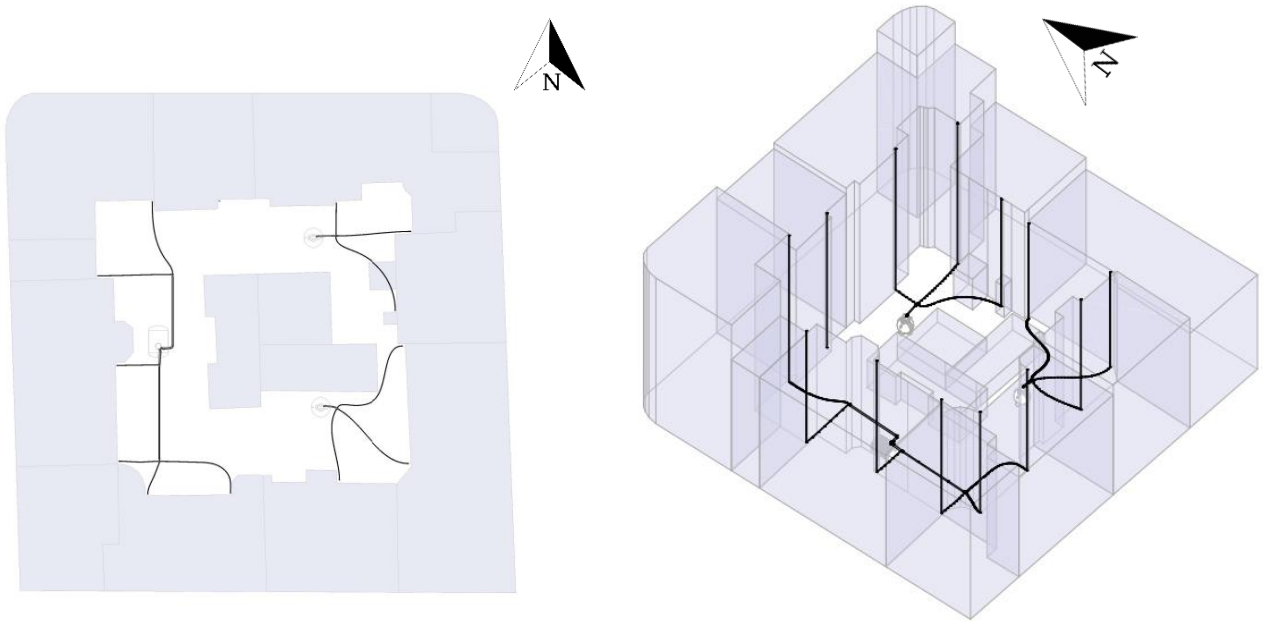

Fig. 16 | Schematic layout of downpipes and underground tanks for the Class 5 building block under traditional roof scenario. The layout is illustrative and does not represent a fully engineered system

For the green roof scenario, runoff from roof sections that remain with a traditional cover is not considered in the analysis. This is due to the lack of reliable data on the distribution of occupants and water demand among individual buildings, as well as the uncertainty in assigning specific roof areas to particular downpipes. Under these conditions, including additional runoff sources would introduce a level of detail and assumptions that is not justified for an academic-scale assessment and would not significantly improve the robustness of the results.

Based on the representative performance curve (Fig. 17), achieving 80% of the maximum E_{WS} efficiency (18.5%) requires a total tank volume of 26 m^3, which is more than twice lower than the storage volume required for a traditional roof. The maximum achievable E_{WS} for the green roof scenario is 23%.

However, the performance curve shows that by sacrificing only 4% of efficiency, the required tank volume can be reduced to 10 m^3, representing a significantly more compact and cost-effective solution.

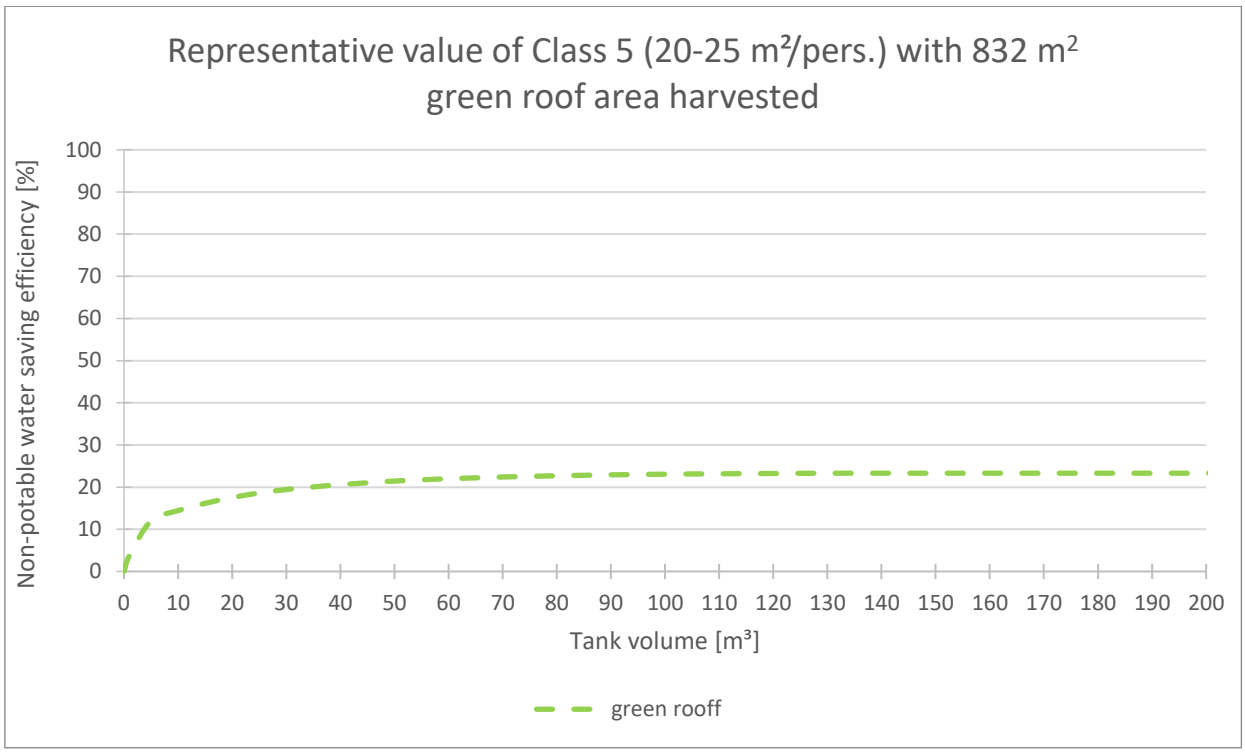

Fig. 17 | Non-potable water savings efficiency E_{WS} for the Class 5 building block under the green roof scenario

The same principle of proportional tank capacity distribution is applied. Accordingly, a 6.2 m³ water tank is placed near the first zone, and a 4.2 m³ tank near the second zone to collect and store runoff from the green roofs.

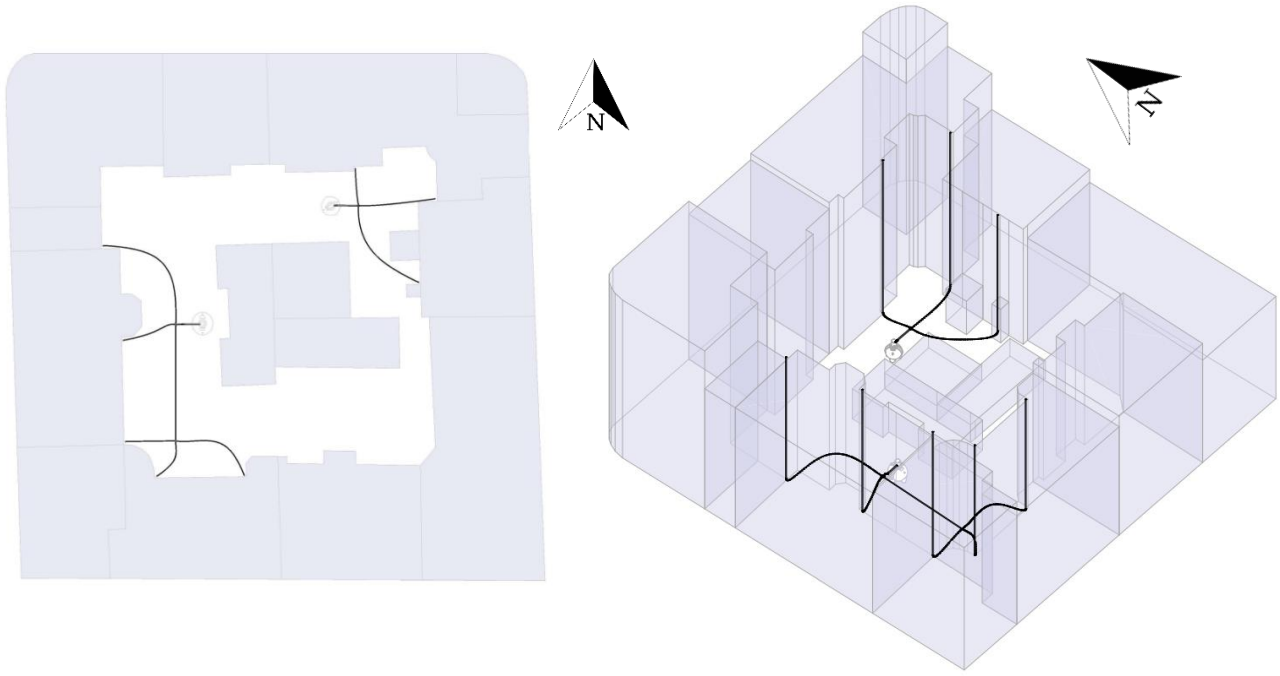

Fig. 18 | Schematic layout of downpipes and underground tanks for the Class 5 building block under green roof scenario. The layout is illustrative and does not represent a fully engineered system

3.4. Economic assessment

To evaluate the yearly economic performance of the proposed RWH system, we can estimate the cost of energy required for pumping and compare it with avoided potable water costs.

The annual pumping energy demand is calculated as:

$$E_{annual} = \frac{\gamma \Delta H V_{annual}}{\eta \cdot 3.6 \cdot 10^6} \quad (8)$$

where γ – specific weight of water; ΔH – total dynamic head; V_{annual} – average annual volume of harvested non-potable water equal to the annual pumped volume); η – pump efficiency (assume equal to 0.6); $3.6 \cdot 10^6$ – conversion factor from Joules to kWh.

Although several tanks are present, each theoretically requiring an individual pump, they were treated as an equivalent single system. This simplification was used because elevation differences and pipe layouts are comparable.

The total head represents the sum of the elevation head, hydraulic losses and the residual head required at the point of use:

$$\Delta H = (z_f - z_i) + \Delta H_M + \Delta H_m + H_{req} \quad (9)$$

where z_f – final elevation at the point of use (toilet connection) for the most disadvantaged user (the farthest location); z_i – initial elevation at the rainwater tank outlet; ΔH_M – major losses due to pipe friction; ΔH_m – minor losses due to fittings, bends, valves, and junctions; H_{req} – required residual head at the device.

The average elevation of roof base if 23.49 m. Consider that connection to toilets is 2 m below the roof level and that the connector to water tank outlet is 0.3 m below ground level, we get the geodetic head is approximated as:

$$z_f - z_i \approx 23.49 - 2.00 - 0.30 = 21.19 \text{ m}.$$

A detailed pipe network design was not feasible due to the absence of internal floor layouts. Therefore, hydraulic losses were estimated using the unit linear head loss method described by Doninelli.

This method assumes that the available unit head is distributed between continuous and localized losses, allowing both to be evaluated together:

$$\Delta H_M + \Delta H_m = J_{tot} = 1.43 \cdot J \cdot L \quad (10)$$

The formulation is derived by assuming that the design value of the unit head loss Jcorresponds, on average, to 70% of the total available unit head J_{TOT}. This fraction represents the portion of energy effectively expended to overcome distributed losses (pipe friction) as well as localized losses caused by fittings, bends, junctions, and diameter variations.

For pressurized domestic systems, recommended values are:

$$80 \leq J \leq 120 \text{ mm c.a./m}$$

These values represent a compromise between installation cost, noise and water hammer control, and acceptable pressure variation across the network.

A mid-range value was adopted:

$$J = 100 \text{ mm/m} = 0.1 \text{ m/m}$$

Since the exact routing is unknown, an equivalent pipe length was assumed as the vertical rise plus an additional 10 m to represent horizontal distribution:

$$L = 21.19 + 10 = 31.19 \text{ m}$$

Thus:

$$\Delta H_M + \Delta H_m = J_{tot} = 1.43 \cdot 0.1 \cdot 31.19 \ = 4.46 \text{ m}$$

For the toilet with a flushing cistern (gravity-fed flush), a residual pressure head according to UNI EN 806-4:2010:

$$H_{req} = 5 \text{ m}$$

And the total dynamic head becomes:

$$\Delta H = \ 21.19 + 4.46 + 5 \ = 30.65 \text{ m}$$

To calculate the annual pumping operation cost, a reference electricity tariff was adopted based on the national regulatory framework defined by ARERA Electrical Energy tariffs 2026.

For February 2026, the indicative single-rate electricity price is:

$$c_e = 0.137 \text{ €/kWh}$$

The annual pumping cost is therefore calculated as:

$$C_{annual} = E_{annual} \cdot c_e \quad (11)$$

According to the tariff structure defined by ARERA for the Integrated Water Service 2025, condominium users are billed on the basis of consumed water volume and the number of dwelling units (unità abitative).

According to the census data from ISTAT, 2021 this building block consists of 135 dwelling units.

From distributing the volume across all apartments, the equivalent consumption per dwelling is:

$$V_{unit} = 500/135 = 3.7\ m^3/(dwelling/year)$$

This value lies entirely within the first tariff tier, which corresponds to the subsidized residential range. Therefore, a unit water price of:

$$c_w = 0.6179€/m^3$$

was adopted for the avoided potable water volume.

It should be noted that the Italian tariff system is progressive; however, the present calculation isolates only the volume replaced by rainwater (toilet flushing). The remaining domestic uses (drinking, cooking, washing, laundry, etc.) are not included here and would normally contribute to higher tariff blocks. Consequently, the adopted unit cost represents a conservative assumption, as the marginal value of substituted potable water could be higher in real conditions.

The annual cost of potable water in the absence of the RWH system can therefore be estimated as:

$$C_{water} = V_{annual} \cdot c_w \quad (12)$$

Scenario I. Traditional roof equipped with rainwater storage tanks with summary volume of 19.4 m^3. In this situation we have the average annual harvested water volume is equal to $V_{annual}^{trad} = 499.2\ m^3$.

$$E_{annual}^{trad} = \frac{\gamma \Delta H V_{annual}^{trad}}{\eta \cdot 3.6 \cdot 10^6} = \frac{9.81 \cdot 10^3 \cdot 30.65 \cdot 499.2}{0.6 \cdot 3.6 \cdot 10^6} = 69.50\ kWh$$

$$C_{energy\ annual}^{trad} = E_{annual}^{trad} \cdot c_e = 69.50 \cdot 0.137 \approx 10\ €/year$$

$$C_{water\ annual}^{trad} = V_{annual}^{trad} \cdot c_w = 499.2 \cdot 0.6179 \approx 308.45\ €/year$$

Scenario II. Green roof equipped 10.4 m^3 water tank. And $V_{annual}^{green} = 268.5\ m^3$.

$$E_{annual}^{green} = \frac{\gamma \Delta H V_{annual}^{green}}{\eta \cdot 3.6 \cdot 10^6} = \frac{9.81 \cdot 10^3 \cdot 30.65 \cdot 268.5}{0.6 \cdot 3.6 \cdot 10^6} = 37.38\ kWh$$

$$C_{energy\ annual}^{green} = E_{annual}^{green} \cdot c_e = 37.38 \cdot 0.137 \approx 6\ €/year$$

$$C_{water\ annual}^{green} = V_{annual}^{green} \cdot c_w = 268.5 \cdot 0.6179 \approx 165.91\ €/year$$

4. DISCUSSION OF THE RESULTS

The results of this study illustrate the potential of rainwater harvesting (RWH) in residential building blocks of Turin, highlighting the influence of roof type, tank capacity, and roof area per inhabitant ratio on system performance. Using the representative building blocks selected for Classes 3, 4, and 5, the analysis estimates both non-potable water savings (E_{WS}) and rainwater retention efficiency (E_R) for traditional and green roof scenarios. The conceptual real-scale design of RWH gives ideas about practical application of such system in the existing urban environment. The economic assessment demonstrates the long-term benefits of RWH systems mainly through savings on water costs.

Non-potable water savings are strongly dependent on the ratio of roof area per capita (H_{pc}). Building blocks with larger roof-to-inhabitant ratios, such as the Class 5 representative block (22.04 m^2/person), achieve the highest E_{WS}, while smaller ratios, like representative block of Class 3 (12.18 m^2/person), show more limited water savings. This confirms that population density is a key factor in the performance of RWH systems, as districts characterized by low-rise buildings and larger roof surfaces per inhabitant generally provide more favorable conditions for rainwater collection. Across all classes, traditional roofs consistently outperform green roofs in terms of water-saving efficiency due to lower initial retention; green roofs, by retaining a portion of rainfall within the substrate and evapotranspiring it, reduce the volume available for collection into tank. For smaller tank volumes, the difference between traditional and green roofs is moderate, but as storage capacity increases, the water-saving efficiency gap widens, reflecting decreasing profit for green roofs under high-volume storage scenarios in terms of non-potable water saving efficiency.

Retention efficiency (E_R), on the other hand, shows an opposite trend. Green roofs significantly improve rainwater retention by absorbing water in substrate layer and plants. Traditional roofs, although achieving higher water savings, retain less rainwater overall, as most of the runoff is directed immediately to the storage tank or sewer system. For traditional roof it is impossible to achieve 100% retention efficiency due to the presence of first flush, directly discharging into sewerage system, which maintains water quality. The representative Class 5 block again exhibits the highest retention efficiencies, followed by Classes 4 and 3, confirming the critical role of roof area per inhabitant ratio in both non-potable water replacement by rainwater and stormwater mitigation.

Overall, the findings reveal a clear trade-off between maximizing non-potable water savings and enhancing stormwater retention. Traditional roofs favor water reuse, while green roofs improve runoff management. Urban planners and building

designers can use these results to prioritize system objectives: optimizing potable water substitution, reducing peak flows, or improving resilience to local storm events.

The conceptual real-scale design for the Class 5 representative block demonstrates practical application of RWH systems in dense urban environment. In the traditional roof scenario, we assumed only roof surfaces sloping towards the inner courtyard. Tank sizing simulations for this value of available roof area indicate that a total storage volume of 20 m^3 is sufficient to achieve approximately 27% E_{WS}, slightly below the 32% optimal threshold, but offering a cost-effective and installable solution. The proposed design places water tanks underground to preserve the courtyard usability, reduce visual impact, protect collected water from temperature fluctuations, and allow gravity-based collection from roof downpipes. For proposing design, we also took into account the existing constraints inside the courtyard, including the presence of low-rise buildings and partitions dividing the space into three zones, which may correspond to different ownerships. As a result, it is not feasible to install a single 20 m^3 storage tank in the center and connect all roof downpipes from surrounding buildings to it, which would be the ideal configuration. Another preferable design option would be to connect the tanks in series at their base to allow water exchange and improve efficiency; however, as we use prefabricated tanks in this study, such connection is not feasible. The prefabricated double-walled polyethylene tanks from the Austrian company Geoplast were selected for design.

In practice, we distributed the required volume across 3 tanks, with capacities proportional to the harvested roof area contributing to them through downpipes. Need to note, that in reality the exact amount of water collected by each downpipe and delivered to the certain tank cannot be determined, and the water demand satisfied by each tank is also unknown, as the number of residents in each building can vary depending on the building's height and layout. Therefore, the previous assumption were introduced for academic purposes.

For the green roof scenario, we have limitations in the form of windows on the upper floors and solar panels on the roof. So only roof areas without them can be considered for installation of green roofs. In this scenario, runoff from roof sections that remain with a traditional cover is not considered in the analysis, this is due to the lack of reliable data on the distribution of occupants and water demand among individual buildings, as well as the uncertainty in assigning specific roof areas to particular downpipes. From tank sizing simulation, the 80% (18.5%) of the maximum E_{WS} efficiency (23%) requires a total tank volume of 26 m^3, which is more than twice lower than the storage volume required for a traditional roof. However, by sacrificing only 4% of efficiency, the required tank volume can be reduced to

10 m^3, representing a significantly more compact and cost-effective solution. The same principle of proportional tank capacity distribution is applied. Accordingly, a 6.2 m^3 water tank is placed near the first zone, and a 4.2 m^3 tank near the second zone to collect and store runoff from the green roofs.

The study suggests the possible design that takes into account the typical constraints of residential blocks in Turin, including separated courtyard space, existing roof features such as windows and solar panels.

In terms of economic assessment of the system, the comparison between the scenarios with and without the RWH system highlights that the main economic benefit comes from avoided potable water costs rather than from energy consumption. Even though the water price is within the subsidized range, the annual cost difference is significant: using the RWH system reduces water expenses from approximately 308 €/year to 10–16 €/year for pumping energy and further reduces potable water demand. The pumping energy demand is negligible because the system operates intermittently and conveys limited volumes over moderate heads typical of residential buildings.

It should be noted that the largest expenses for an RWH system are related to the installation of tanks and pumps, as well as potential maintenance. Nevertheless, the substantial reduction in potable water costs demonstrates that, over time, the system can provide meaningful economic savings while promoting sustainable water management at the building scale.

The proposed methodology, combining GIS-based spatial analysis with behavioral modeling, proves effective for evaluating RWH performance at building block scale and offer a practical tool for RWH systems design.

5. LITERATURE

1. Carollo M, Butera I, Revelli R (2022) Water savings and urban storm water management: Evaluation of the potentiality of rainwater harvesting systems from the building to the city scale. PLoS ONE 17(11):e0278107. https://doi.org/10.1371/journal.pone.0278107
2. Sousa V, Carollo M, Butera I, Meireles I (2025) The combined performance of green roof and rainwater harvesting: retention capacity and water saving. Blue-Green Systems Vol 7 No 1, 238. https://doi.org/10.2166/bgs.2025.041
3. Campisano A, Butler D, Ward S, Burns MJ, Friedler E, DeBusk K et al (2017) Urban rainwater harvesting systems: Research, implementation and future perspectives. Water Research 115:195–209. https://doi.org/10.1016/j.watres.2017.02.056
4. Notaro V, Liuzzo L, Freni G (2016) Reliability analysis of rainwater harvesting systems in Southern Italy. Procedia Eng 162:373–380. https://doi.org/10.1016/j.proeng.2016.11.077
5. GhaffarianHoseini A, Tookey J, GhaffarianHoseini A, Yusoff SM, Hassan NB (2016) State of the art of rainwater harvesting systems towards promoting green built environments: A review. Desalination and Water Treatment 57:95–104. https://doi.org/10.1080/19443994.2015.1021097
6. Campisano A, Modica C (2014) Selecting time scale resolution to evaluate water saving and retention potential of rainwater harvesting tanks. Procedia Engineering 70:218–227. https://doi.org/10.1016/j.proeng.2014.02.025
7. Campisano A, Modica (2015) Appropriate resolution timescale to evaluate water saving and retention potential of rainwater harvesting for toilet flushing in single houses. Journal of Hydroinformatics 17(3):331–346. https://doi.org/10.2166/hydro.2015.022
8. Palla A, Gnecco I, Lanza LG, La Barbera P (2012) Performance analysis of domestic rainwater harvesting systems under various European climate zones. Resources, Conservation and Recycling 62:71–80. https://doi.org/10.1016/j.resconrec.2012.02.006
9. Jenkins GA (2007) Use of continuous simulation for the selection of an appropriate urban rainwater tank. Australasian Journal of Water Resources 11(2). https://doi.org/10.1080/13241583.2007.11465327
10. Imteaz MA, Paudel U, Ahsan A, Santos C (2015) Climatic and spatial variability of potential rainwater savings for a large coastal city. Resources,

Conservation & Recycling 105:143–147. https://doi.org/10.1016/j.resconrec.2015.10.023

11. Lúcio C, Silva CM, Sousa V (2020) A scale-adaptive method for urban rainwater harvesting simulation. Environmental Science and Pollution Research 27:4557–4570. https://doi.org/10.1007/s11356-019-04889-6
12. Islam MM, Afrin S, Tarek MH, Rahman MM (2021) Reliability and financial feasibility assessment of a community rainwater harvesting system considering precipitation variability due to climate change. J Environ Manage 289:112507. https://doi.org/10.1016/j.jenvman.2021.112507
13. United Nations (2015) Transforming our world: the 2030 Agenda for Sustainable Development. United Nations General Assembly A/RES/70/1. https://docs.un.org/en/A/RES/70/1
14. Leong JYC, Oh KS, Poh PE, Chong MN (2017) Prospects of hybrid rainwater-greywater decentralised system for water recycling and reuse: A review. Journal of Cleaner Production 142:3014–3027. https://doi.org/10.1016/j.jclepro.2016.10.152
15. Palla A, Gnecco I, Lanza LG (2011) Non-dimensional design parameters and performance assessment of rainwater harvesting systems. J Hydrol (Amst) 401:65–76. https://doi.org/10.1016/j.jhydrol.2011.02.009
16. Zanni S, Cipolla SS, di Fusco E, Lenci A, Altobelli M, Currado A, Maglionico M, Bonoli A (2019) Modeling for sustainability: Life cycle assessment application to evaluate environmental performance of water recycling solutions at the dwelling level. Sustainable Production and Consumption 17:47–61. https://doi.org/10.1016/j.spc.2018.09.002
17. Fewkes A, Butler D (2000) Simulating the performance of rainwater collection and reuse systems using behavioural models. Build Serv Eng Res Technol 21(2):99–106. https://doi.org/10.1177/014362440002100204
18. Guo Y, Baetz BW (2007) Sizing of rainwater storage units for green building applications. J Hydrol Eng 12(2):197–205. https://doi.org/10.1061/(ASCE)1084-0699(2007)12:2(197)
19. Raimondi A, Becciu G (2014) Probabilistic modeling of rainwater tanks. Procedia Eng 89:1493–1499. https://doi.org/10.1016/j.proeng.2014.11.437
20. Silva CM, Sousa V, Carvalho NV (2015) Evaluation of rainwater harvesting in Portugal: Application to single-family residences. Resour Conserv Recycl 94:21–34. https://doi.org/10.1016/j.resconrec.2014.11.004

21. Ghisi E, Ferreira DF (2007) Potential for potable water savings by using rainwater and greywater in a multi-story residential building in southern Brazil. Build Environ 42:2512–22. https://doi.org/10.1016/j.buildenv.2006.07.019

22. Mitchell VG, Deletic A, Fletcher TD, Hatt BE, McCarthy DT (2007) Achieving multiple benefits from stormwater harvesting. Water Sci Technol 55:135–44. https://doi.org/10.2166/wst.2007.103

23. Brodie I (2012) Stormwater harvesting and WSUD frequent flow management: A compatibility analysis. Water Sci Technol 66:612–19. https://doi.org/10.2166/wst.2012.214

24. Campisano A, Modica C (2012) Optimal sizing of storage tanks for domestic rainwater harvesting in Sicily. Resour Conserv Recycl 63:9–16. https://doi.org/10.1016/j.resconrec.2012.03.007

25. Campisano A, Gnecco I, Modica C, Palla A (2013) Designing domestic rainwater harvesting systems under different climatic regimes in Italy. Water Sci Technol 67:2511–18. https://doi.org/10.2166/wst.2013.143

26. Ente nazionale italiano di unificazione (UNI) (2012) UNI/TS 11445, Impianti per la raccolta e utilizzo dell'acqua piovana per usi diversi dal consumo umano. Progettazione, installazione e manutenzione. Milan: UNI.

27. Farreny R, Morales-Pinzón T, Guisasola A, Tayà C, Rieradevall J, Gabarrell X (2011) Roof selection for rainwater harvesting: quantity and quality assessments in Spain. Water Res 45(10):3245–54. https://doi.org/10.1016/j.watres.2011.03.036

28. Kus B, Kandasamy J, Vigneswaran S, Shon H (2010) Analysis of first flush to improve the water quality in rainwater tanks. Water Sci Technol 61(2):421–8. https://doi.org/10.2166/wst.2010.823

29. Amin MT, Kim T-I, Amin MN, Han MY (2013) Effects of catchment, first-flush, storage conditions, and time on microbial quality in rainwater harvesting systems. Water Environ Res 85:2317–29. https://doi.org/10.2175/106143013X13706200598433

30. Silva AS, Ghisi E (2016) Uncertainty analysis of daily potable water demand on the performance evaluation of rainwater harvesting systems in residential buildings. J Environ Manage 180:82–93. https://doi.org/10.1016/j.jenvman.2016.05.028

31. Silva MMM, Maia AG (2021) Equation for rainwater tank efficiency: Considering demand, roof area, tank size and pluvial regime. Environ Chall 3:100044. https://doi.org/10.1016/j.envc.2021.100044

32. Mitchell VG, McCarthy DT, Deletic A, Fletcher TD (2008) Urban stormwater harvesting – sensitivity of a storage behaviour model. Environ Model Softw 23:782–793. https://doi.org/10.1016/j.envsoft.2007.09.006

33. ISTAT. Basi territoriali e variabili censuarie. https://www.istat.it/notizia/basi-territoriali-e-variabili-censuarie/

34. Ghisi E, Bressan DL, Martini M (2007) Rainwater tank capacity and potential for potable water savings by using rainwater in the residential sector of southeastern Brazil. Build Environ 42:1654–1666. https://doi.org/10.1016/j.buildenv.2006.02.007

35. Mitchell VG (2007) How important is the selection of computational analysis method to the accuracy of rainwater tank behaviour modelling? Hydrol Process 21(21):2850–61. https://doi.org/10.1002/hyp.6499

36. Palermo SA, Turco M, Principato F, Piro P (2019) Hydrological effectiveness of an extensive green roof in Mediterranean climate. Water 11:1378. https://doi.org/10.3390/w11071378

37. Dixon A, Butler D, Fewkes A (1999) Water saving potential of domestic water reuse systems using greywater and rainwater in combination. Water Sci Technol 38(4):25–32. https://doi.org/10.1016/S0273-1223(99)00083-9

38. Beck HE, McVicar TR, Vergopolan N, Berg A, Lutsko NJ, Dufour A, Zeng Z, Jiang X, van Dijk AIJM, Miralles DG (2023) High-resolution (1 km) Köppen-Geiger maps for 1901–2099 based on constrained CMIP6 projections. Sci Data 10:724. https://doi.org/10.1038/s41597-023-02549-6

39. Commissione parlamentare di inchiesta sulle condizioni di sicurezza e sullo stato di degrado delle città e delle loro periferie. Report Comune di Torino. Roma, 26 giugno 2024. ISTAT. https://www.istat.it/wp-content/uploads/2024/06/Approfondimento_Torino.pdf

40. Società Metropolitana Acque Torino (SMAT) (2025) Bilancio consolidato e bilancio dell'esercizio 2024. Approvato dall'Assemblea Ordinaria dei Soci in data 25/06/2025. https://www.smatorino.it/wp-content/uploads/2025/07/BILANCIO-SMAT-31-12-2024-light.pdf

41. Geraldi MS, Ghisi E (2018) Assessment of the length of rainfall time series for rainwater harvesting in buildings. Resour Conserv Recycl 133:231–241. https://doi.org/10.1016/j.resconrec.2018.02.007

42. Agudelo-Vera CM, Keesman KJ, Mels AR, Rijnaarts HHM (2013) Evaluating the potential of improving residential water balance at building scale. Water Res 47(20):7287–7299. https://doi.org/10.1016/j.watres.2013.10.040

43. Basinger M, Montalto F, Lall U (2010) A rainwater harvesting system reliability model based on nonparametric stochastic rainfall generator. J Hydrol 392:105–118. https://doi.org/10.1016/j.jhydrol.2010.07.039

44. Herrmann T, Schmida U (2000) Rainwater utilisation in Germany: efficiency, dimensioning, hydraulic and environmental aspects. Urban Water 1(4):307–316. https://doi.org/10.1016/S1462-0758(00)00024-8

45. Villarreal EL, Dixon A (2005) Analysis of a rainwater collection system for domestic water supply in Ringdansen, Norrköping, Sweden. Build Environ 40(9):1174–1184. https://doi.org/10.1016/j.buildenv.2004.10.018

46. Ghisi E, Cardoso KA, Rupp RF (2012) Short-term versus long-term rainfall time series in the assessment of potable water savings by using rainwater in houses. J Environ Manage 100:109–119. https://doi.org/10.1016/j.jenvman.2011.12.031

47. Geraldi MS, Ghisi E (2017) Influence of the length of rainfall time series on rainwater harvesting systems: A case study in Berlin. Resour Conserv Recycl 125:169–180. https://doi.org/10.1016/j.resconrec.2017.06.011

48. World Meteorological Organization (WMO) (1989) Calculation of Monthly and Annual 30-year Standard Normals. Geneva: WMO, Technical Document No. 341; WCDP No. 10.

49. Moniruzzaman M, Imteaz MA (2017) Generalized equations, climatic and spatial variabilities of potential rainwater savings: A case study for Sydney. Resour Conserv Recycl 125:139–156. https://doi.org/10.1016/j.resconrec.2017.06.001

50. Domeisen DIV, Butler AH, Fröhlich K, Bittner M, Müller WA, Baehr J (2015) Seasonal predictability over Europe arising from El Niño and stratospheric variability in the MPI-ESM seasonal prediction system. J Clim 28:256–271. https://doi.org/10.1175/JCLI-D-14-00207.1

51. IPCC (2007) Climate change 2007: impacts, adaptation and vulnerability. Contribution of working group II to the fourth assessment report of the

intergovernmental panel on climate change. Cambridge University Press, Cambridge, UK.

52. Lehner B, Döll P, Alcamo J, Henrichs T, Kaspar F (2006) Estimating the impact of global change on flood and drought risks in Europe: a continental, integrated analysis. Clim Chang 75:273–299. https://doi.org/10.1007/s10584-006-6338-4

53. Frich P, Alexander LV, Della-Marta P, Gleason B, Haylock M, Tank Klein AMG, Peterson T (2002) Observed coherent changes in climatic extremes during the second half of the twentieth century. Clim Res 19:193–212. https://doi.org/10.3354/cr019193

54. Klein Tank AMG, Wijngaard JB, Können GP, Böhm R, Demarée G, Gocheva A, Mileta M, Pashiardis S, Hejkrlik L, Kern-Hansen C, Heino R, Bessemoulin P, Müller-Westermeier G, Tzanakou M, Szalai S, Pálsdóttir T, Fitzgerald D, Rubin S, Capaldo M, Maugeri M, Leitass A, Bukantis A, Aberfeld R, Van Engelen AFV, Forland E, Mietus M, Coelho F, Mares C, Razuvaev V, Nieplova E, Cegnar T, Antonio López J, Dahlström B, Moberg A, Kirchhofer W, Ceylan A, Pachaliuk O, Alexander LV, Petrovic P (2002) Daily dataset of 20th-century surface air temperature and precipitation series for the European climate assessment. Int J Climatol 22:1441–1453. https://doi.org/10.1002/joc.773

55. ARPA Piemonte. Rete meteorologica. Disponibile su: https://www.arpa.piemonte.it/rischi_naturali/snippets_arpa_graphs/map_meteoweb/?rete=stazione_meteorologica

56. ARPA Piemonte. Carta del suolo. Disponibile su: https://webgis.arpa.piemonte.it/agportal/apps/webappviewer/index.html?id=6ea1e38603d6469298333c2efbc76c72

57. ARPA Piemonte. Monitoraggio della qualità delle acque, corpo idrico GWB-S3b, punto 00127210001, Comune di Torino. Disponibile su: https://webgis.arpa.piemonte.it/monitoraggio_qualita_acque/indexpiez.php?numcodice=00127210001

58. Geoplast S.p.A (2025) Rainwater tanks catalogue. Geoplast sustainable water storage solutions including polyethylene underground tanks for rainwater harvesting, retention and infiltration, with modular configurations and accessories. Available at: https://www.geoplast.com/de/produkte?f%5B0%5D=kategorien%3A155

59. Doninelli M, Doninelli M, Cremona E, Crimella A, Godi M, Mazzetti D, Planca R, Tomasoni M (2016) Le reti di distribuzione degli impianti

idrosanitari. Idraulica, Pubblicazione periodica di informazione tecnico-professionale 50, Caleffi S.p.A., Fontaneto d'Agogna, Italy. https://www.caleffi.com/sites/default/files/media/external-file/Idraulica_50_IT_Le%20reti%20di%20distribuzione%20degli%20impianti%20idrosanitari%20.pdf

60. UNI EN 806-4:2010. Specifiche relative agli impianti all'interno di edifici per il convogliamento di acque destinate al consumo umano.
61. luce-gas.it. Guida alle tariffe elettriche: prezzi e costi dell'energia elettrica per uso domestico e civile. Available at: https://luce-gas.it/guida/tariffe/kwh
62. ARERA (2025) Articolazione tariffaria per il Servizio Idrico Integrato – Anno 2025. Available at: https://www.smatorino.it/wp-content/uploads/2025/01/Tariffe-2025.pdf

APPENDIX A

Table A.1 | Characteristics of residential building blocks in the study area

BUILDING BLOCK ID	№ RESIDENTS [INHAB.]	№ DWELLINGS [UNITS]	№ RESIDENTIAL BUILDINGS [UNITS]	№ ALL BUILDINGS [UNITS]	TOTAL ROOF AREA [M2]	ROOF AREA/INHAB. [M2/PERS.]	CLASS	AVG. DAILY POTABLE WATER DEMAND [M3]	AVG. DAILY NON-POTABLE WATER DEMAND [M3]
1147	95	135	4	5	2093.84	22.04	5	15.11	5.04
1148	163	137	8	10	2846.74	17.46	4	25.92	8.64
1149	157	115	6	7	2536.00	16.15	4	24.96	8.32
1150	357	274	14	19	5493.80	15.39	4	56.76	18.92
1151	97	125	11	17	2730.50	28.15	6	15.42	5.14
1152	48	26	3	3	1552.77	32.35	7	7.63	2.54
1153	340	273	11	13	4594.54	13.51	3	54.06	18.02
1154	128	100	8	13	2615.28	20.43	5	20.35	6.78
1155	232	192	15	20	5087.82	21.93	5	36.89	12.30
1156	310	229	20	22	5750.67	18.55	4	49.29	16.43
1158	219	84	7	13	4833.17	22.07	5	34.82	11.61
1159	310	206	10	13	6964.65	22.47	5	49.29	16.43
1160	180	163	15	18	3462.21	19.23	4	28.62	9.54
1161	241	161	10	13	4347.99	18.04	4	38.32	12.77
1162	149	112	6	10	3697.79	24.82	5	23.69	7.90
1163	292	230	18	23	5785.74	19.81	4	46.43	15.48
1164	56	57	5	7	1315.43	23.49	5	8.90	2.97
1165	313	191	14	24	5331.49	17.03	4	49.77	16.59
1166	240	146	11	12	5014.25	20.89	5	38.16	12.72
1167	250	170	12	14	3885.20	15.54	4	39.75	13.25
1168	216	138	9	14	4573.04	21.17	5	34.34	11.45
1169	176	130	10	20	5063.00	28.77	6	27.98	9.33
1170	291	277	9	9	5698.63	19.58	4	46.27	15.42
1171	208	206	12	15	3462.26	16.65	4	33.07	11.02

Table A.1 – Continued | Characteristics of residential building blocks in the study area

1172	279	202	17	23	5508.80	19.74	4	44.36	14.79
1173	223	126	10	16	4488.43	20.13	5	35.46	11.82
1174	81	48	2	4	1802.37	22.25	5	12.88	4.29
1175	237	200	12	18	4631.32	19.54	4	37.68	12.56
1176	241	198	16	22	4711.69	19.55	4	38.32	12.77
1177	346	201	5	6	5324.05	15.39	4	55.01	18.34
1178	300	256	9	12	4729.72	15.77	4	47.70	15.90
1180	271	189	17	21	4921.26	18.16	4	43.09	14.36
1181	142	118	4	6	2340.18	16.48	4	22.58	7.53
1182	180	203	18	24	4873.71	27.08	6	28.62	9.54
1183	247	166	11	16	4286.25	17.35	4	39.27	13.09
1184	254	163	7	8	2835.63	11.16	3	40.39	13.46
1185	375	280	17	21	6487.48	17.30	4	59.63	19.88
1186	238	157	16	21	4624.58	19.43	4	37.84	12.61
1187	287	158	10	12	4727.12	16.47	4	45.63	15.21
1188	274	240	11	11	2816.55	10.28	3	43.57	14.52
1189	217	175	13	14	3565.22	16.43	4	34.50	11.50
1190	60	55	4	4	864.99	14.42	3	9.54	3.18
1191	624	510	37	48	11234.69	18.00	4	99.22	33.07
1192	188	137	8	10	2801.39	14.90	3	29.89	9.96
1193	293	173	18	22	4536.99	15.48	4	46.59	15.53
1194	104	150	4	4	1868.35	17.96	4	16.54	5.51
1195	592	413	30	39	7211.83	12.18	3	94.13	31.38
1197	427	312	19	23	6980.65	16.35	4	67.89	22.63
3256	106	108	3	3	1965.98	18.55	4	16.85	5.62
3257	77	40	3	4	1346.14	17.48	4	12.24	4.08
3258	228	129	7	7	2738.13	12.01	3	36.25	12.08
5896	207	147	12	15	3587.38	17.33	4	32.91	10.97